



**POLITECNICO**  
MILANO 1863

SCUOLA DI INGEGNERIA INDUSTRIALE  
E DELL'INFORMAZIONE

# Quantum Information-Theoretic Analysis of DNA Communication: Channel Capacity, Decomposition, and Synthesis

TESI DI LAUREA MAGISTRALE IN  
TELECOMMUNICATION ENGINEERING - INGEGNERIA DELLE  
TELECOMUNICAZIONI

Author: **Alessandro Barbaro**

Student ID: 996516

Advisor: Prof. Maurizio Magarini

Co-advisors:

Academic Year: 2024-25



# Abstract

Just as quantum physics generalizes classical physics, quantum information theory extends Shannon's classical information theory, introducing a vast array of tools that make it suitable for analyzing and processing information in quantum systems. Its applications also extend to the description of biological processes that are believed to possess an intrinsic quantum nature, potentially exploiting non-trivial quantum effects — such as tunneling and superposition — to enhance their efficiency. At the same time, significant efforts are being devoted to the development of quantum computers, with the goal of building reliable machines capable of simulating complex quantum processes. In this thesis, referring to previous studies that modeled the transfer of genetic information between DNA and proteins as a quantum communication system, we show how the introduction of quantum coherence between codons that encode for the same protein leads to a gain of mutual information between DNA and proteins with respect to the classical case. We give a description of the quantum biological channel as a convex combination of extreme channels that permit to build a quantum circuit with a limited number of CNOT gates. Finally, we perform a Monte Carlo simulation to demonstrate the asymptotic convergence of the capacity evaluated through the quantum circuit implementation to the theoretical value.

**Keywords:** quantum information theory, quantum biology, DNA, protein synthesis, quantum circuits, biological channel capacity.



# Abstract in lingua italiana

Così come la fisica quantistica generalizza la fisica classica, la teoria dell'informazione quantistica estende la teoria classica di Shannon, introducendo strumenti che permettono di analizzare e processare l'informazione nei sistemi quantistici. Le sue applicazioni si estendono anche alla descrizione di processi biologici che si ritiene abbiano una natura intrinsecamente quantistica, potenzialmente sfruttando effetti quantistici non banali, come il tunneling e la sovrapposizione, per aumentarne l'efficienza. In questa tesi, basandoci su studi precedenti che modellano il trasferimento di informazione genetica tra DNA e proteine come un sistema di comunicazione quantistico, mostriamo come l'introduzione di coerenza quantistica tra codoni che codificano per la stessa proteina porti a un incremento dell'informazione mutua tra DNA e proteine rispetto al caso classico. Descriviamo il canale biologico quantistico come combinazione convessa di canali estremi che consente la costruzione di un circuito quantistico con un numero contenuto di porte CNOT. Infine, eseguiamo una simulazione Monte Carlo per mostrare la convergenza asintotica della capacità calcolata tramite il circuito ai risultati teorici.

**Parole chiave:** informazione quantistica, biologia quantistica, DNA, sintesi proteica, circuiti quantistici, capacità canale biologico.



# Contents

<b>Abstract</b>	<b>i</b>
<b>Abstract in lingua italiana</b>	<b>iii</b>
<b>Contents</b>	<b>v</b>
<b>Introduction</b>	<b>1</b>
<b>1 Theoretical background</b>	<b>3</b>
1.1 Useful mathematics . . . . .	3
1.1.1 Linear algebra . . . . .	3
1.1.2 Graph theory . . . . .	4
1.2 A Short introduction to quantum mechanics . . . . .	6
1.2.1 The postulates of quantum mechanics . . . . .	6
1.2.2 The density operator . . . . .	7
1.3 Quantum circuits . . . . .	8
1.3.1 Single and controlled qubit operations . . . . .	8
1.3.2 Universal quantum gates . . . . .	10
1.4 Quantum operations . . . . .	10
1.5 Quantum information . . . . .	12
1.5.1 Von Neumann entropy . . . . .	12
1.5.2 The Holevo bound and the HSW theorem . . . . .	13
1.6 The structure of DNA and the genetic information . . . . .	14
<b>2 Quantum biological information theory</b>	<b>19</b>
2.1 Quantum aspects of DNA . . . . .	19
2.2 Quantum biological channel model for DNA flow of information . . . . .	20
2.2.1 The classical communication model with noisy channel . . . . .	20

2.2.2	The quantum communication model . . . . .	23
2.2.3	Operator-sum representation and capacity evaluation of the noisy quantum channel . . . . .	26
2.3	Alternative quantum biological channel for DNA flow of information . . . .	30
2.3.1	Channel convex decomposition . . . . .	31
2.3.2	Capacity evaluation assuming coherence at the protein side . . . . .	34
<b>3</b>	<b>Quantum circuit for quantum biological channel</b>	<b>35</b>
3.1	Circuit construction . . . . .	35
3.2	Capacity evaluation . . . . .	42
<b>4</b>	<b>Conclusions</b>	<b>45</b>
	<b>Bibliography</b>	<b>47</b>
<b>A</b>	<b>Appendix A</b>	<b>49</b>
<b>B</b>	<b>Appendix B</b>	<b>51</b>
<b>C</b>	<b>Appendix C</b>	<b>53</b>
<b>D</b>	<b>Appendix D</b>	<b>57</b>
	<b>List of Figures</b>	<b>59</b>
	<b>List of Tables</b>	<b>61</b>
	<b>Acknowledgements</b>	<b>63</b>

# Introduction

The twentieth century was a time when many scientific contributions have been made in order to have a deeper understanding about many aspects of human beings and in general, of nature. From the vast landscape of knowledge, quantum physics and biology have been two of the main protagonists of scientific debate. The former describes the very peculiar characteristics of nature at the nanoscale level, while biology is known as the science that studies life. The interest in the connection of these two disciplines, now known as quantum biology, started when Erwin Schrödinger wrote in 1944 the booklet "What is life?" [13] where he pointed out that some aspects of life such as heredity and mutations must be significantly dependent on the quantum phenomena, since they are governed by the stability of the genes that, according to him, can only be explained from a quantum perspective. In 1953, Watson and Crick uncovered the structure of DNA. Soon afterward, authors such as [9, 10] noticed that the proton involved in hydrogen bonds between the nitrogenous bases joining the two DNA strands might occasionally shift, producing mutations. This is because, due to the wave-packet nature of quantum particles, the proton can jump from one side to the other of the bond due to tunneling. In parallel, other theories have been born and grown. Information theory for example, was used by Yockey [17] and applied to the "central dogma of molecular biology" to model the transfer of information from DNA to proteins as a classical communication channel. He represented the DNA as a source of information with an alphabet of 64 symbols (codons) and the receiver as one of the 20 amino acids determined by the codons. Assuming a noisy channel, he computed the mutual information between DNA and proteins as a function of the error introduced by the channel. More recently, a quantum characterization of the same problem was done by Karafyllidis [8] and a definition of a noisy channel and the capacity calculation of such a system was done by Djordjevic [3]. Our contribution will be that of giving a representation of the same quantum system but with a more practical spirit, pushing towards the possibility of simulating such a system with the forthcoming quantum computers.

The thesis is organized as follows. In Chapter 1 we present the background theory essential

for understanding the following chapters. In the first part of Chapter 2 we give a historical background of the key developments in the description of the DNA–protein information flow in both classical and quantum terms. We then present our main contributions. In particular:

- In the second part of Chapter 2 we show that the channel defined by Djordjevic can be decomposed into a convex combination of extreme quantum channels, enabling a more straightforward synthesis of the corresponding quantum dynamics in terms of elementary quantum gates.
- In the same section we demonstrate that the quantum model proposed by Karafyllidis increases the mutual information between DNA and proteins compared to the classical case.
- In Chapter 3 we show one of the many possible ways to implement the quantum map of the first point in a quantum circuit. In particular, we will exploit the method of the Householder reflections according to [11], showing that the CNOT count of the circuit is proportional to  $(18n - 26)(2^n - 1)$ , where  $n$  is the number of qubits of the system. A numerical analysis for the evaluation of the channel capacity through the quantum circuit will also be presented.

# 1 | Theoretical background

In this chapter, we summarize the theoretical tools needed to properly understand the problems discussed in the following chapters. We review some algebraic results that are useful for handling the quantum formalism; we introduce some concepts from graph theory that will turn out to be very useful; we provide an overview of the quantum tools required to describe quantum systems and quantum channels; and finally, we introduce some basic concepts about DNA and its structure.

## 1.1. Useful mathematics

### 1.1.1. Linear algebra

In quantum mechanics an *observable* is a physical quantity (for example energy, momentum etc.) that can be measured. An observable can be represented by a linear *operator* [12], that is, a linear function  $A : V \rightarrow W$ , where  $V$  and  $W$  are vector spaces:

$$A \left( \sum_i a_i |v_i\rangle \right) = \sum_i a_i A(|v_i\rangle). \quad (1.1)$$

The most convenient way to understand operators is in terms of their equivalent *matrix representation*. In fact a matrix  $A$  with entries  $a_{i,j}$  sending vectors in the vector space  $\mathbf{C}^n$  to the vector space  $\mathbf{C}^m$  under matrix multiplication of the matrix  $A$  by a vector on  $\mathbf{C}^n$ , is a linear operator. We can then write equation (1.1) as:

$$A \left( \sum_i a_i |v_i\rangle \right) = \sum_i a_i A |v_i\rangle. \quad (1.2)$$

Here are some useful assertions.

- A *diagonal representation* for an operator  $A$  on a vector space  $V$  is a representation

$A = \sum_i \lambda_i |i\rangle \langle i|$ , where the vectors  $|i\rangle$  form an orthonormal set of eigenvectors for  $A$ , with the corresponding eigenvalues  $\lambda_i$ . An operator is said to be *diagonalizable* if it has a diagonal representation.

- An operator is said to be *Hermitian* if  $A^\dagger = A$ , where  $A^\dagger = (A^T)^*$ .
- An operator  $A$  is said to be *normal* if  $AA^\dagger = A^\dagger A$ . An operator which is Hermitian is also normal.
- *Theorem 1.1 (spectral decomposition)*: Any normal operator  $M$  on a vector space  $V$  is diagonal with respect to some orthonormal basis for  $V$ . Conversely, any diagonalizable operator is normal.
- An operator  $U$  is unitary if  $U^\dagger U = I$ . A unitary operator also satisfies  $UU^\dagger = I$ , so  $U$  is also normal and has a spectral decomposition.

### 1.1.2. Graph theory

A graph is constituted by two elements: vertices and edges. An example of a graph is represented in Figure 1.1. We can call this graph  $G$ . The set of vertices is  $\mathcal{V} = \{a, b, c, d, e, f\}$  while the set of edges is  $\mathcal{D} = \{ab, ac, bd, dc, de, ef\}$ .

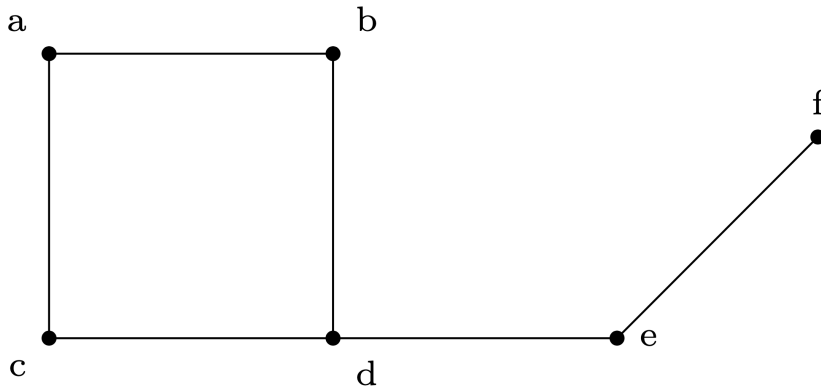


Figure 1.1: Graph  $G$  with six vertices and six edges

A *matching* is a set of edges with no two adjacent edges in the set. Two edges are adjacent if they share the same common-end vertex. As an example, for the graph  $G$  we can define the matching  $M_1 = \{ac, ef\}$ . A *maximal matching* of a graph is a matching that is not a subset of any other matching. In our case  $M_1$  is not maximal because by adding the edge  $bd$ , we get a bigger matching, i.e.,  $M_2 = \{ac, ef, bd\}$ .  $M_2$  is a maximal matching because is not a subset of a bigger matching: we cannot increase the cardinality of  $M_2$

by adding another edge. A *maximum matching* is a matching that contains the largest possible number of edges. In our example  $M_2$  is maximum and maximal at the same time. In this graph there is another matching  $M_3 = \{ab, cd, ef\}$  that has the same properties as  $M_2$ . Not every maximal matching is a maximum matching. For example  $M_4 = \{de, ac\}$  is a maximal matching but not a maximum matching. A *perfect matching* is a match such that any vertex in the graph is incident with an edge in the matching. If we have a matching, a sub-graph induced by the matching will be a *bipartite graph*, i.e., a graph whose vertices can be divided into two distinct and independent sets, with every edge connecting a vertex in one set to a vertex in the other set.

We now state an important theorem that will be useful later for the existence of perfect matchings.

*Theorem 1.2 (Hall's condition):*

Let  $G = (X, Y, D)$  a bipartite graph with bipartite sets  $X$  and  $Y$ . For a subset  $W$  of  $X$ , let  $N_G(W)$  denote the neighborhood of  $W$  in  $G$ , the set of all vertices in  $Y$  that are adjacent to at least one element of  $W$ . Then there is an  $X$ -perfect matching if and only if for every subset of  $W$  of  $X$ :

$$|W| \leq |N_G(W)| \quad (1.3)$$

In other words, every subset  $W$  of  $X$  must have sufficiently many neighbors in  $Y$ .

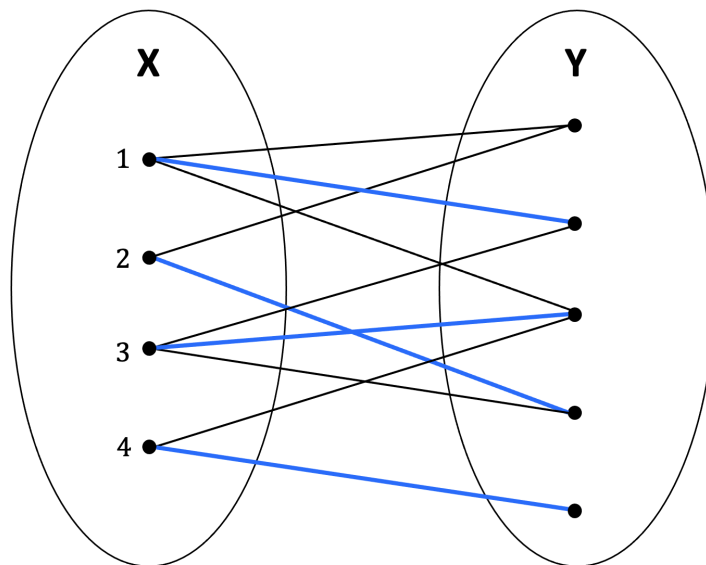


Figure 1.2: Example of bipartite graph. Blue edges represent a perfect matching

A perfect matching on a bipartite graph can be found using the Hopcroft-Karp algorithm [6].

## 1.2. A Short introduction to quantum mechanics

In this section we are referring to [12] for the discussion of the postulates of quantum mechanics and the equivalent representation of the state of a quantum system in terms of density operator.

### 1.2.1. The postulates of quantum mechanics

**Postulate 1:** Associated with any isolated physical system is a complex vector space with inner product (that is, a Hilbert space) known as the *state space* of the system. The system is completely described by its *state vector*, which is a unit vector in the state space of the system.

The simplest quantum mechanical system is the *qubit*. A qubit is a two dimensional Hilbert and we define  $|0\rangle$  and  $|1\rangle$  as the canonical orthonormal base for the state space. Then the general state vector in the state space can be written as

$$|\psi\rangle = \alpha |0\rangle + \beta |1\rangle \quad (1.4)$$

where  $\alpha$  and  $\beta$  are complex numbers. To satisfy the unitary condition, the scalar product  $\langle\psi|\psi\rangle = 1$ , leading to  $a^2 + b^2 = 1$ .

**Postulate 2:** The evolution of a closed quantum system is described by a unitary transformation. This means that the state  $|\psi\rangle$  of the system at time  $t_1$  is related to the state  $|\psi'\rangle$  of the system at time  $t_2$  by a unitary operator  $U$  which depends only on the times  $t_1$  and  $t_2$ ,

$$|\psi'\rangle = U |\psi\rangle. \quad (1.5)$$

**Postulate 3:** Quantum measurements are described by a collection  $\{M_m\}$  of *measurement operators*. These are operators acting on the state space of the system being measured. The index  $m$  refers to the measurement outcomes that may occur in the experiment. If

the state of the quantum system is  $|\psi\rangle$  immediately before the measurement then the probability that result  $m$  occurs is given by:

$$p(m) = \langle\psi| M_m \rho M_m^\dagger |\psi\rangle \quad (1.6)$$

and the state of the system after the measurement is

$$\frac{M_m |\psi\rangle}{\sqrt{\langle\psi| M_m^\dagger M_m |\psi\rangle}}. \quad (1.7)$$

The measurement operator satisfies the *completeness equation*

$$\sum_m M_m^\dagger M_m = I. \quad (1.8)$$

The completeness relation ensures that probabilities sum up to one.

**Postulate 4:** The state space of a composite physical system is the tensor product of the state spaces of the component physical systems. If we have systems numbered 1 through  $n$ , and system number  $i$  is prepared in the state  $|\psi_i\rangle$ , then the joint state of the total system is  $|\psi_1\rangle \otimes |\psi_2\rangle \otimes \dots \otimes |\psi_n\rangle$ . For details about the mathematics of composite systems see [2, ch. II.F]

### 1.2.2. The density operator

An alternative way, but very often useful, to describe quantum systems is the *density operator*. The density operator provides a convenient way to describe a quantum system whose state is not completely known. Suppose we have a system that can be in one of the states  $|\psi_i\rangle$  with probabilities  $p_i$ . We call  $\{|\psi_i\rangle, p_i\}$  an ensemble of pure states. The density operator for the system is defined as

$$\rho \equiv \sum_i p_i |\psi_i\rangle \langle\psi_i|. \quad (1.9)$$

All the postulates we have defined before can be reformulated in terms of density operator language [12, Sec. 2.4.1]. A quantum system whose state  $|\psi\rangle$  is known exactly is said to be a *pure state* and the density operator is  $\rho = |\psi\rangle \langle\psi|$ . Otherwise, just as before,

the system is said to be a *mixture* of different pure states of the ensemble and  $\rho$  is a *mixed state*. A useful mathematical characterization of the density operator is given by the following theorem:

*Theorem 1.3:* An operator  $\rho$  is the density operator associated to some ensemble  $\{|\psi_i\rangle, p_i\}$  if and only if it satisfies the following conditions:

1. (**Trace condition**)  $\rho$  has trace equal to one;
2. (**Positivity condition**)  $\rho$  is a positive operator.

*Corollary 1.1:* let  $\rho$  a density operator. Then  $\text{tr}(\rho^2) \leq 1$ , with equality if and only if  $\rho$  is a pure state.

As an example, consider the qubit system in a state  $|\psi\rangle = \alpha|0\rangle + \beta|1\rangle$ . Its squared density operator is

$$\rho^2 = |\psi\rangle\langle\psi| |\psi\rangle\langle\psi| = |\psi\rangle\langle\psi| = \begin{bmatrix} |a|^2 & a^*b \\ b^*a & |b|^2 \end{bmatrix}, \quad (1.10)$$

than for the normalization condition  $\text{tr}(\rho^2) = |a|^2 + |b|^2 = 1$ , showing that  $|\psi\rangle$  is a pure state.

### 1.3. Quantum circuits

The implementation of a general unitary operator  $U$  on a quantum system of  $n$  qubits is a very important operation in quantum computing. A general  $U$  acting on a  $n$  qubit closed system represents most of the possible transformations that we can perform on the system. In order to implement the unitary on quantum hardware, we have to decompose it into elementary single- and two-qubit gates. In this section we will see a very essential overview of the elementary building blocks of quantum circuits.

#### 1.3.1. Single and controlled qubit operations

We have already seen that the simplest quantum system is the qubit. A general state in this system is described by a unitary vector on a 2-dimensional Hilbert space  $|\psi\rangle = \alpha|0\rangle + \beta|1\rangle$ . Operations on a qubit system must preserve norm, and thus are described by  $2 \times 2$  unitary matrices. Of these, some of the most important are the *Pauli matrices* and the *Hadamard gate*  $H$ :

$$X \equiv \begin{bmatrix} 0 & 1 \\ 1 & 0 \end{bmatrix}; \quad Y = \begin{bmatrix} 0 & -i \\ i & 0 \end{bmatrix}; \quad Z = \begin{bmatrix} 1 & 0 \\ 0 & -1 \end{bmatrix}; \quad H = \frac{1}{\sqrt{2}} \begin{bmatrix} 1 & 1 \\ 1 & -1 \end{bmatrix}. \quad (1.11)$$

There are many interesting and useful results in the field of single-qubit operations that derive from the combination of the matrices mentioned above. For this work they are not essential, but if interested check [12, Sec. 4.2].

Other very important operations are the *controlled operations*. A fundamental controlled operation is the controlled-NOT or CNOT. It is a quantum gate with two input qubits known as the *control qubit* and *target qubit*. See Figure 1.3 for the circuit representation. In terms of computational basis the action of the CNOT is  $|c\rangle|t\rangle \rightarrow |c\rangle|t \oplus c\rangle$ ; that is if the control qubit is set to  $|1\rangle$  then the target qubit is flipped, otherwise the target is unchanged. In the computational basis the CNOT is represented as:

$$CNOT = |0\rangle\langle 0| \otimes I + |1\rangle\langle 1| \otimes X = \begin{bmatrix} 1 & 0 & 0 & 0 \\ 0 & 1 & 0 & 0 \\ 0 & 0 & 0 & 1 \\ 0 & 0 & 1 & 0 \end{bmatrix}. \quad (1.12)$$

Note that the CNOT cannot be written in separable form  $A \otimes B$  otherwise no interactions between target and control qubit would occur.

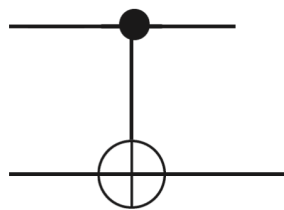


Figure 1.3: Circuit representation for the controlled-NOT gate. The top line represents the control qubit, the bottom line the target qubit.

More generally, suppose that we have  $n + k$  qubits and  $U$  is a  $k$  qubit unitary operator. Then we can define the controlled operation  $C^n(U) |x_1 x_2 \dots x_n\rangle |\psi\rangle = |x_1 x_2 \dots x_n\rangle U^{x_1 x_2 \dots x_n} |\psi\rangle$  where the exponent of  $U$   $x_1 x_2 \dots x_n$  is the product of the bits  $x_1, x_2, \dots, x_n$ . The operator  $U$  is then applied to the last  $k$  qubits if the first  $n$  are equal to one, otherwise nothing is done. In Figure 1.4 is represented an example with  $n = 4$  and  $k = 3$ .

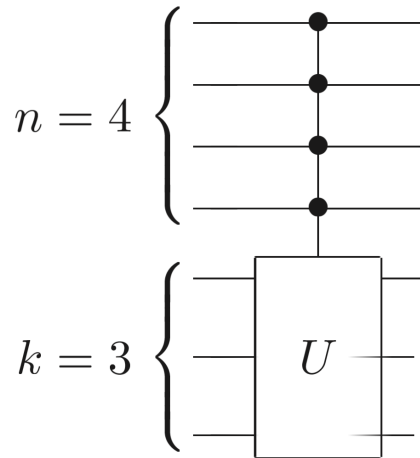


Figure 1.4: Circuit representation for the  $C^n(U)$  operation, where  $U$  is a unitary operator on  $k$  qubits, for  $n = 4$  and  $k = 3$ .

In this work we will use only multi-controlled target qubit, i.e., with  $k = 1$

### 1.3.2. Universal quantum gates

As we have already said, quantum computing corresponds, abstractly, to implementing a general unitary on a set of qubits system. The aim of the circuit model for quantum computation is to break down the unitary in terms of a small family of simple-to-perform gates. As in classical computing there are small sets of gates (for instance AND, OR, NOT) that can be used to compute arbitrary classical functions; a similar result is true for quantum computation where a set of gates is said to be *universal for quantum computation*, if any unitary operation may be approximated to arbitrary accuracy by a quantum circuit involving only those gates.

## 1.4. Quantum operations

The way of how to describe the dynamical change of quantum systems goes under the name of *quantum operations*. In the simple case where the change of closed systems is described by unitary transformations  $U$ , we know that the new state of the system will be  $U|\psi\rangle$  - if  $|\psi\rangle$  is the state of the system before having applied the transformation. We can also use the density operator notation and give a description of the system after the unitary transformation as  $U\rho U^\dagger$  where  $\rho = |\psi\rangle\langle\psi|$ . In addition to unitary transformation, we shall also include measurements  $M_m$  as operators that can change the quantum system without

destroying it, and thus making it available for further experiments after its interaction. In fact, in this case if the result  $m$  occurs, the new state will be:

$$\rho_m = \frac{M_m \rho M_m^\dagger}{\text{tr}(M_m \rho M_m^\dagger)}. \quad (1.13)$$

Other types of dynamical changes are the open ones, where the system of interest, the principal system, interacts with another system, the environment, which together form a closed quantum system, as illustrated in Figure 1.5.

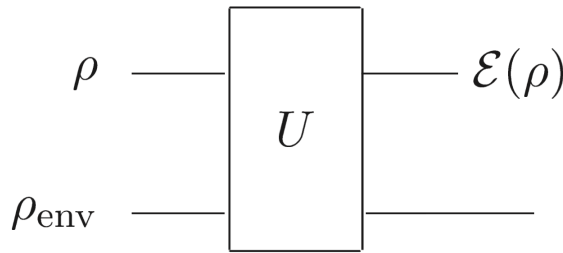


Figure 1.5: Open quantum system consists of principal system and environment

We define a mapping  $\mathcal{E} : \rho \rightarrow \rho'$  where from the initial state of the principal system, we get the final state:

$$\mathcal{E}(\rho) = \text{tr}_E[U(\rho \otimes \rho_E)U^\dagger]. \quad (1.14)$$

We then suppose that the closed composite quantum system made by the principal system and the environment, which initially are in separable form (they do not interact), are unitary transformed by  $U$ , making in general interactions between the two subsystems and, to retrieve only the principal subsystem we trace out the environment. If we assume, without loss of generality, that the initial state of the environment is a pure state  $\rho_E = |e_0\rangle\langle e_0|$  and that the set  $\{e_k\}$  is an orthonormal basis for the (finite-dimensional) state space of the environment, applying the property of the trace, (1.14) can be rewritten as:

$$\mathcal{E}(\rho) = \sum_k \langle e_k | U(\rho \otimes |e_0\rangle\langle e_0|) U^\dagger | e_k \rangle = \sum_k E_k \rho E_k^\dagger. \quad (1.15)$$

The last equality represents the quantum operation in the so-called operator-sum representation and the elements  $E_k = \langle e_k | U | e_0 \rangle$  are called *Kraus operators* which act only on

the state space of the principal system and represent, individually, one of the possible actions on the initial system due to the interaction with the environment. We can interpret  $\text{tr}(E_k \rho E_k^\dagger)$  as the transition probability for the transition map  $\mathcal{E}_k(\rho) = E_k \rho E_k^\dagger$  and so:

$$\text{tr}(\mathcal{E}(\rho)) = \sum_k \text{tr}(\mathcal{E}_k(\rho)) = \text{tr}\left(\sum_k E_k \rho E_k^\dagger\right) = \text{tr}\left(\sum_k E_k^\dagger E_k \rho\right) = 1 \quad (1.16)$$

Since this relation is valid for all  $\rho$ , we must have  $\sum_k E_k^\dagger E_k = I$ . More generally  $\sum_k E_k^\dagger E_k \leq I$  and if equality holds, we are in the case of quantum operations that are *trace-preserving*.

As an example suppose that we have an open qubit system that is interacting with the environment, initialized at the state  $|0_e\rangle$ , via the Pauli  $X$  operator. Namely  $U = \sqrt{p}I \otimes I + \sqrt{1-p}X \otimes X$  and we take  $|\psi_e\rangle |\psi_s\rangle$ . This operator acts on the state environment in the following way:

$$U |0_e\rangle = (\sqrt{p}I \otimes I) |0_e\rangle + (\sqrt{1-p}X \otimes X) |0_e\rangle = \sqrt{p} |0_e\rangle I + \sqrt{1-p} |1_e\rangle X.$$

We can derive the Kraus operators

$$E_0 = \langle 0_e | U | 0_e \rangle = \sqrt{p}I; \quad E_1 = \langle 0_e | U | 1_e \rangle = \sqrt{1-p}X,$$

which describes the following interaction: there is a probability  $p$  that nothing happens to the qubit, while there is a probability  $1-p$  that there is a bit flip error. The quantum operation is:

$$\mathcal{E}(\rho) = p\rho + (1-p)X\rho X^\dagger.$$

## 1.5. Quantum information

### 1.5.1. Von Neumann entropy

As the Shannon entropy gives a measure of the uncertainty of the random variable defined by its probability distribution, the Von Neuman entropy gives a measure of the uncertainty of the quantum state defined by its density operator. For a quantum state  $\rho$  the Von Neuman entropy is defined as:

$$S(\rho) \equiv -\text{tr}(\rho \log \rho), \quad (1.17)$$

where the logarithm is taken to base two. If  $\lambda_x$  are the eigenvalues of  $\rho$  then, we can express the quantum entropy also as:

$$S(\rho) = - \sum_x \lambda_x \log \lambda_x, \quad (1.18)$$

where we define  $0 \log 0 \equiv 0$ .

*Theorem 1.4 (Von Neuman entropy properties):*

1. the entropy is non-negative. The entropy is zero if and only if the state is pure;
2. in a  $d$ -dimensional Hilbert space the entropy is at most  $\log d$ . The entropy is equal to  $\log d$  if and only if the system is in the completely mixed state  $I/d$ ;
3. for a mixture  $\sum_i p_i \rho_i$  of quantum states  $\rho_i$  the following inequality holds:

$$\sum_i p_i S(\rho_i) \leq S\left(\sum_i p_i \rho_i\right) \leq \sum_i p_i S(\rho_i) + H(p_i). \quad (1.19)$$

Left inequality holds if and only if all states  $\rho_i$  are identical; right inequality holds if and only if the states  $\rho_i$  have support on orthogonal subspaces.

### 1.5.2. The Holevo bound and the HSW theorem

A very important result in quantum information is the *Holevo bound*. It says how much information we can get from a classical source if its messages have been encoded in quantum states. We know that from a classical source we cannot get more information than its uncertainty  $H(X)$ , i.e., than the information that the source itself can give. In the quantum field things are a little bit more complicated since quantum states can be intrinsically indistinguishable. The Holevo bound is the quantity that takes into account the hidden information that non-orthogonal states keep, limiting the accessible information, i.e., the maximum information we can extract from the classical source  $X$ .

*Theorem 1.5 (The Holevo bound):*

Suppose that Alice prepares a state  $\rho_X$  where  $X = 0, \dots, n$  with probabilities  $p_0, \dots, p_n$ .

Bob performs a measurement described by POVM elements  $\{E_y\} = \{E_0, \dots, E_m\}$  on that state, with measurement outcome  $Y$ . The Holevo bound states that for any such measurement Bob may do:

$$H(X : Y) \leq S(\rho) - \sum_x p_x S(\rho_x), \quad (1.20)$$

where  $\rho = \sum_x p_x \rho_x$  and  $H(X : Y)$  is the mutual information between  $X$  and  $Y$ .

Another important result in quantum information that we will use later for the evaluation of the quantum biological channel capacity is the Holevo–Schumacher–Westmoreland (HSW) theorem. The idea, as in classical communication, is that we would evaluate the maximum rate at which classical messages, encoded in quantum states, can reliably sent through a quantum noisy channel.

*Theorem 1.6 (Holevo–Schumacher–Westmoreland (HSW) theorem):*

let  $\mathcal{E}$  be a trace-preserving quantum operation. Define

$$C(\mathcal{E}) \equiv \max_{\{p_j, \rho_j\}} \left[ S \left[ \mathcal{E} \left( \sum_j p_j \rho_j \right) \right] - \sum_j p_j S(\mathcal{E}(\rho_j)) \right] \quad (1.21)$$

where the maximum is over all ensembles  $\max\{p_j, \rho_j\}$  of possible input states  $\rho_j$  to the channel

## 1.6. The structure of DNA and the genetic information

DNA (deoxyribonucleic acid) is an extremely large molecule relative to the size of the cell nucleus in which it resides [16]. It carries the genome, that is, the information required to specify the physical structure of an organism and it is written using four bases (called nucleotides): A-adenine, T-thymine, C-cytosine and G-guanine. The DNA molecule consists of a double helix formed by two strands held together by a sequence of base pairs A-T or C-G as depicted In Figure 1.7. This particular structure of DNA facilitates its *replication*: during the cell division process the DNA must duplicate itself and give one copy to the daughter cell. In order to do this, the double helix starts unwinding and at the same time each stand starts to build its own complement giving rise to two identical DNA molecules containing the original genetic information; see Figure 1.7. The unwind-

ing of DNA is not necessary only when the cell must divide. It is also necessary when proteins must be synthesized. Proteins are essentially linear structures made of a chain of twenty amino acids and their biochemical properties are determined by the sequence of these amino acids. This sequence is ultimately determined by the base sequence in DNA. DNA itself is not directly involved in making proteins, it must be *transcribed* in a molecule called RNA (ribonucleic acid). Afterward, RNA is *translated* into a sequence of amino acids that give rise to a protein. Such transfers of biological information are summarized by the *central dogma of molecular biology* stated by Francis Crick in 1958 (see figure below).

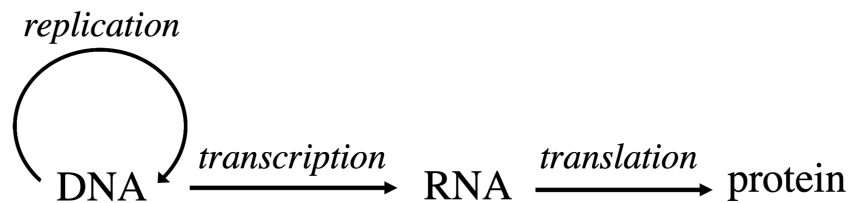


Figure 1.6: Transfer of information from DNA to itself (replication) and from DNA to protein through RNA

RNA is very similar to DNA, but it has the base U instead of T; furthermore, RNA exists mostly in single-strand form. There exist three types of RNA molecules:

1. mRNA (messenger RNA): created after the transcription process, it is the molecule that carries the genetic information in order to synthesize proteins;
2. rRNA: molecules that combine with proteins to form ribosomes, "machines" used to synthesize proteins;
3. tRNA: its function is to collect and bring the proper amino acid to the ribosome so that, the ribosome, can use those amino acids to synthesize the polypeptide chain.

The genetic message is contained in each one of the two DNA strands in complementary form. It is evident that one single nucleotide cannot code for one amino acid since there are 20 different types of the last one and only four nucleotides. In order to specify a single amino acid, a group of bases called *codons* is necessary. A couple of nucleotides is not enough, as we can do only  $4^2$  different doublets. With groups of three nucleotides, we get  $4^3$  and this code permits to specify the same amino acid with different codons. This is the reason why the genetic code is said to be *degenerate*, see Figure 1.8.

The entire sequence of DNA includes genes and non-coding regions and together constitute

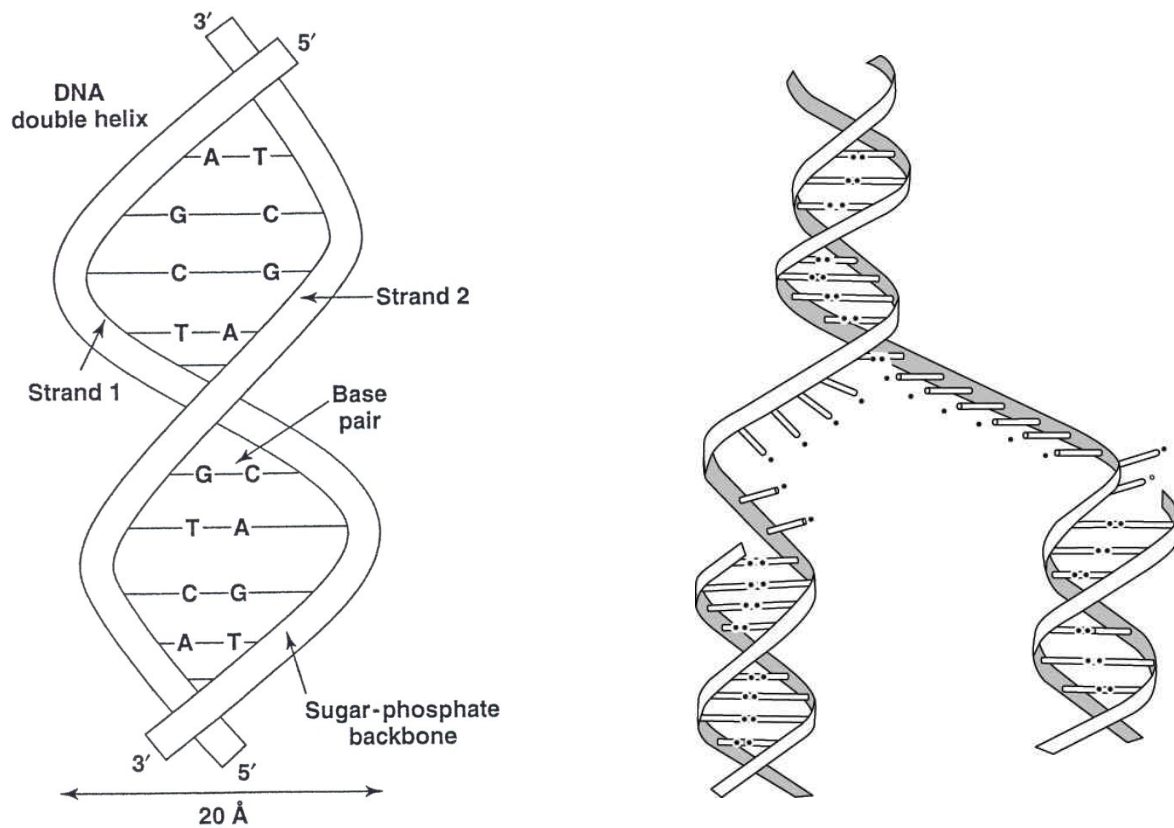


Figure 1.7: On the left, the DNA double-helix structure is illustrated; on the right, the unwinding of DNA during the replication process is shown.

the genome. Only a small percentage of the genome consists of coding regions that code for proteins. Instead rRNA is made only of parts of the genes that contain the information for building proteins. Using directly DNA as a source of information is not efficient because there are many regions meaningless from an information point of view and it is dangerous since it is easy to damage it.

First Base in the Codon	Second Base of the Codon				Third Base in the Codon
	U	C	A	G	
<b>U</b>	<b>UUU</b> Phenylalanine	<b>UCU</b> Serine	<b>UAU</b> Tyrosine	<b>UGU</b> Cysteine	<b>U</b> <b>C</b> <b>A</b> <b>G</b>
	<b>UUC</b> Phenylalanine	<b>UCC</b> Serine	<b>UAC</b> Tyrosine	<b>UGC</b> Cysteine	
	<b>UUA</b> Leucine	<b>UCA</b> Serine	<b>UAA</b> STOP	<b>UGA</b> STOP	
	<b>UUG</b> Leucine	<b>UCG</b> Serine	<b>UAG</b> STOP	<b>UGG</b> Tryptophan	
<b>C</b>	<b>CUU</b> Leucine	<b>CCU</b> Proline	<b>CAU</b> Histidine	<b>CGU</b> Arginine	<b>U</b> <b>C</b> <b>A</b> <b>G</b>
	<b>CUC</b> Leucine	<b>CCC</b> Proline	<b>CAC</b> Histidine	<b>CGC</b> Arginine	
	<b>CUA</b> Leucine	<b>CCA</b> Proline	<b>CAA</b> Glutamine	<b>CGA</b> Arginine	
	<b>CUG</b> Leucine	<b>CCG</b> Proline	<b>CAG</b> Glutamine	<b>CGG</b> Arginine	
<b>A</b>	<b>AUU</b> Isoleucine	<b>ACU</b> Threonine	<b>AAU</b> Asparagine	<b>AGU</b> Serine	<b>U</b> <b>C</b> <b>A</b> <b>G</b>
	<b>AUC</b> Isoleucine	<b>ACC</b> Threonine	<b>AAC</b> Asparagine	<b>AGC</b> Serine	
	<b>AUA</b> Isoleucine	<b>ACA</b> Threonine	<b>AAA</b> Lysine	<b>AGA</b> Arginine	
	<b>AUG</b> Methionine	<b>ACG</b> Threonine	<b>AAG</b> Lysine	<b>AGG</b> Arginine	
<b>G</b>	<b>GUU</b> Valine	<b>GCU</b> Alanine	<b>GAU</b> Aspartic Acid	<b>GGU</b> Glycine	<b>U</b> <b>C</b> <b>A</b> <b>G</b>
	<b>GUC</b> Valine	<b>GCC</b> Alanine	<b>GAC</b> Aspartic Acid	<b>GGC</b> Glycine	
	<b>GUA</b> Valine	<b>GCA</b> Alanine	<b>GAA</b> Glutamic Acid	<b>GGA</b> Glycine	
	<b>GUG</b> Valine	<b>GCG</b> Alanine	<b>GAG</b> Glutamic Acid	<b>GGG</b> Glycine	

Figure 1.8: The genetic code



# 2 | Quantum biological information theory

In this chapter, we introduce the quantum properties that DNA is believed to exhibit according to [9, 10], discussing their biological implications. Building on these considerations, and following a historical path that traces how classical and quantum information theory have been progressively applied to the modeling of the central dogma of molecular biology, we give an alternative description, which turns out to be very useful in the next chapter, of the quantum channel defined by Djoedjevic [3] in extreme quantum channels. Finally, we explore the potential advantages, from an information-theoretic perspective, of considering coherence between similar codons on the protein side.

## 2.1. Quantum aspects of DNA

The interest in the quantum properties of DNA and in general of biological processes began when E. Schrödinger in his little book "What is Life?" (1944) claimed that quantum effects could have an important role in the genetic hereditary problem. In 1953 Watson and Crick discovered the DNA (somehow predicted by Schrödinger, who envisioned that the genetic information would have been in an aperiodic crystal) and since then it has been possible to study microscopically the characteristics of this fundamental molecule for life. An important contribution was due to Löwdin in 1963 [9, 10]. The base pairs of DNA are connected by a hydrogen bond that essentially consists of a proton shared between two electron pairs of two distinct atoms (Figure 2.2). Nucleotides can have different configurations depending on which side of the bond is the proton. These different configurations are called *tautomeric* forms (Figure 2.3). They are obtained by changing the proton position from up to middle or vice versa. We can see that the new electronic configuration of the tautomeric bases leads to a different type of coupling of the different nucleotides: A\* - C, A - C\*, G\* - T, G - T\*. The complementarity between the basis is changed and the movement of a single proton will influence the genetic message and

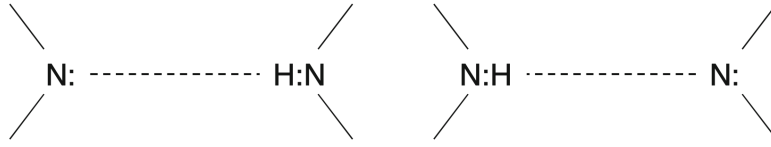


Figure 2.1: Possible positions of the proton shared in the hydrogen bond

introduce an error at the first cell duplication.

The potential felt by the proton shared between the two electron pairs can be modeled as a double-well potential. In this scenario the proton has classically two equilibrium positions, one close to each one of the electron pairs involved as depicted in Figure 2.1. We know that quantum particles can show either corpuscular or wave-like behavior, so the proton can cross the barrier by tunneling effect. The dynamic of the proton inside the double-well potential is regulated by the time-dependent Schrodinger equation

$$H |\psi\rangle = -\frac{\hbar}{2\pi i} \frac{d|\psi\rangle}{dt}. \quad (2.1)$$

It is not hard to find the exact solution of the time dependent wave function (see [10]). Of course the genetic message stored in the DNA is assumed to be highly stable. This means that the double potential cannot be symmetric (in this case we will come out with eigenstates that are a superposition of the two equilibrium states, i.e., the probability of being in one of the two equilibrium states is  $1/2$ ) but highly asymmetric. This model is useful to find the transition probability of the proton to jump in the tautomeric state.

## 2.2. Quantum biological channel model for DNA flow of information

### 2.2.1. The classical communication model with noisy channel

The description of the flow of genetic information according to the central dogma was first studied with the tools of classical communication and information theory by Yockey [17]. He evaluated the capacity of such a channel considering an input alphabet of 61 codons (all  $4^3 = 64$  minus the three stop codons) and an output alphabet of 20 amino acids. He hypothesized, according to experimental data, that the probability distribution of the codons was uniform, leading to an input entropy of  $H_{\text{in}} = \log_2 61 = 5.931$  bits/codon.

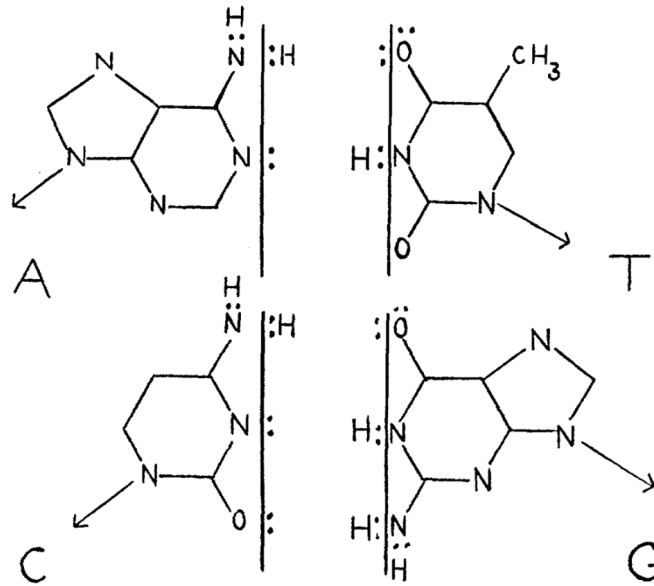


Figure 2.2: Molecular structure of nucleotides. Here the pair A -T has two hydrogen bonds; C - G has three hydrogen bonds.

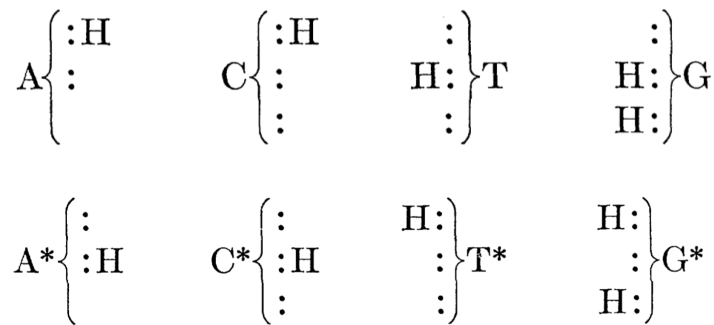


Figure 2.3: The upper figure shows a simplified representation of the nucleotides, illustrating the configuration of hydrogen bonds at the interface under standard conditions; the lower figure depicts their corresponding tautomeric forms.

In the absence of error due to the degeneracy of the code, writing the probability of the  $n$ th amino acid as  $p_n = \sum_m p_{n|m} p_m$ , with  $p_m$  probability of  $m$ th codon, he found that the entropy was  $H_{\text{out}} = 4.139$  bits/residue rather than the maximum:  $\log_2 20 = 4.322$  bits/residue, arguing the biological sense of this. In a standard way he computed the biological channel capacity of the transfer of information from DNA to proteins through the mutual information between codons and proteins:

$$I(X, Y) = H(X) - H(X|Y). \quad (2.2)$$

Of course the maximization over the input distribution is omitted since we are not able (at least without considering genetic engineering) to change the input distribution of codons. Since the distribution of the input alphabet is fixed,  $H(X)$  is also fixed. Due to degeneracy the conditional entropy is not going to zero when the error is null: knowing a specific amino acid we cannot tell exactly which codon has been used to produce that amino acid. The only exception to this is for the amino acids Met and Trp [17]. It is anyway interesting to explicit the conditional entropy  $H(X|Y)$  to really appreciate the degeneracy of this coding scheme. With some simple passages and the Bayes' rule we can rewrite:

$$H(X|Y) = H(Y|X) + \sum_{m,n} p_m p_{n|m} \log_2 \frac{p_n}{p_m}, \quad (2.3)$$

where  $p_n$  is the probability of the  $n$ th amino acid. The second term goes to zero only in case of zero error if there is no degeneracy. It represents the redundant information of the genetic code and it is the information that cannot be transferred from DNA to proteins. In order to compute the general rate, Yockey introduced a transition matrix that maps, with a probability of error proportional to a parameter  $\alpha$ , all 64 codons to the corresponding amino acids of the 21 possible ones, i.e., he considered both stop codons and terminators. One can easily adapt a similar transition matrix to the case of 61 codons and 20 amino acids considering some transition erased. Yockey's work does not show just an application of the information theory on a field different from the one is born: from a different point of view it also confirms the "postulate" of the central dogma. The latter claims that genetic information can flow only from DNA to protein and not vice versa. In fact, since the maximum entropy at the protein side is significantly less than at DNA side, due to this loss of information, it would be impossible to retrieve the information originated in DNA from the proteins.

### 2.2.2. The quantum communication model

For a quantum description of the same problem an important contribution was due Karafyllidis [8]. In the construction of a system describing the flow of information between DNA and proteins, the essential characteristics that must be considered are: the input alphabet, which is made of 64 different and distinguishable codons; the output alphabet, which is made of 20 different and distinguishable amino acids; it must exist a map that associates at each codon an amino acid according to the degenerate map of Figure 1.8. In order to satisfy the first requirement, as in the classical case, DNA is considered as the sender of information, and it is represented by a 64-dimensional Hilbert space on which is defined a Hamiltonian:

$$H_{DNA} = \sum_{m=1}^{61} E_m |m\rangle \langle m|. \quad (2.4)$$

The above equation is the spectral decomposition of the Hermitian observable  $H_{DNA}$  with 61 non-degenerate eigenvalues  $E_m$  and 61 orthogonal eigenvectors  $|m\rangle = |e_1\rangle$  representing each input codon. For the second requirement, on the protein side, a 61-dimensional Hilbert space is still considered. The base states remain the 61 codons but now the eigenvalues are degenerate and grouped, in order to satisfy also the third requirement, according to the degenerate coding scheme:

$$H_{PROT} = \begin{array}{c} |AUG\rangle \\ |UGG\rangle \\ |AAA\rangle \\ |AAG\rangle \\ \vdots \\ |AGC\rangle \\ |AGG\rangle \end{array} \begin{array}{c} |AUG\rangle \\ |UGG\rangle \\ |AAA\rangle \\ |AAG\rangle \\ \cdots \\ |AUG\rangle \\ |AGG\rangle \end{array} \left[ \begin{array}{cccccc} E_1 & 0 & 0 & 0 & \cdots & 0 & 0 \\ 0 & E_2 & 0 & 0 & \cdots & 0 & 0 \\ 0 & 0 & E_3 & 0 & \cdots & 0 & 0 \\ 0 & 0 & 0 & E_3 & \cdots & 0 & 0 \\ \vdots & \vdots & \vdots & \vdots & \ddots & \vdots & \vdots \\ 0 & 0 & 0 & 0 & \cdots & E_{20} & 0 \\ 0 & 0 & 0 & 0 & \cdots & 0 & E_{20} \end{array} \right] \quad (2.5)$$

The structure of  $H_{DNA}$  and  $H_{PROT}$  reflects the action of the channel on the genetic



if they differ in one nucleotide or in two successive nucleotides".

3. "Since nucleotide A has only two hydrogen bond sites, we take into account only the first and second bond sites of all nucleotides. If there is an amplitude between two states and the donor/acceptor pattern of the different nucleotides is the same, then the amplitude is  $ia$ , where  $i$  is the imaginary unit. If the donors and acceptors are interchanged, then the amplitude is  $a$ ".

As an example, we will consider the block matrix corresponding to the only amino acid encoded by three codons: Ile. Following the assumptions the block  $B_{12}$  is:

$$B_{12} = \begin{bmatrix} E_{\text{Ile}} & a & a \\ a & E_{\text{Ile}} & ia \\ a & -ia & E_{\text{Ile}} \end{bmatrix}. \quad (2.7)$$

Solving the Schrodinger stationary equation  $B_{12} |\text{Ile}\rangle = E |\text{Ile}\rangle$  we end up with the eigenvalues  $E_{\text{Ile}}$  and  $E_{\text{Ile}} \pm \sqrt{3}$ , and eigenvectors:

$$\begin{aligned} |\text{Ile}^{(1)}\rangle &= \frac{1}{\sqrt{3}}(-i |\text{AUU}\rangle - |\text{AUA}\rangle + |\text{AUC}\rangle); \\ |\text{Ile}^{(2)}\rangle &= \frac{1}{\sqrt{3}} \left( \frac{1}{2}(i - \sqrt{3}) |\text{AUU}\rangle - \frac{1}{2}(i\sqrt{3} - 1) |\text{AUA}\rangle + |\text{AUC}\rangle \right); \\ |\text{Ile}^{(3)}\rangle &= \frac{1}{\sqrt{3}} \left( \frac{1}{2}(i + \sqrt{3}) |\text{AUU}\rangle + \frac{1}{2}(i\sqrt{3} + 1) |\text{AUA}\rangle + |\text{AUC}\rangle \right). \end{aligned}$$

It is easy to check that these eigenstates are orthonormal. For a full derivation of all the block matrices see [3, 8].

It is interesting to note that with new assumptions at the protein side, the code is no more degenerate and there are 61 different eigenvalues corresponding to 20 amino acids. It would be interesting to know if such quantum representation can somehow have a better behavior in terms of information. Clearly knowing one out of 61 eigenvalues can not tell much about what was sent. For instance, obtaining as a measure, at the protein side, the value  $E_{\text{Ile}} + \sqrt{3}$ , we can tell that the state has collapsed on the eigenket  $|\text{Ile}^{(3)}\rangle$ , that is, a state that is generated with probability  $1/3$  by all the three codons corresponding to the amino acid Ile. This argument can be extended for all the other cases except for those amino acids that are encoded by families of six codons: arginine, leucine and serine. In this case not all codons can collapse in all the six eigenkets, i.e., it is possible to gain extra information knowing which eigenvalue has been measured or in which state the system

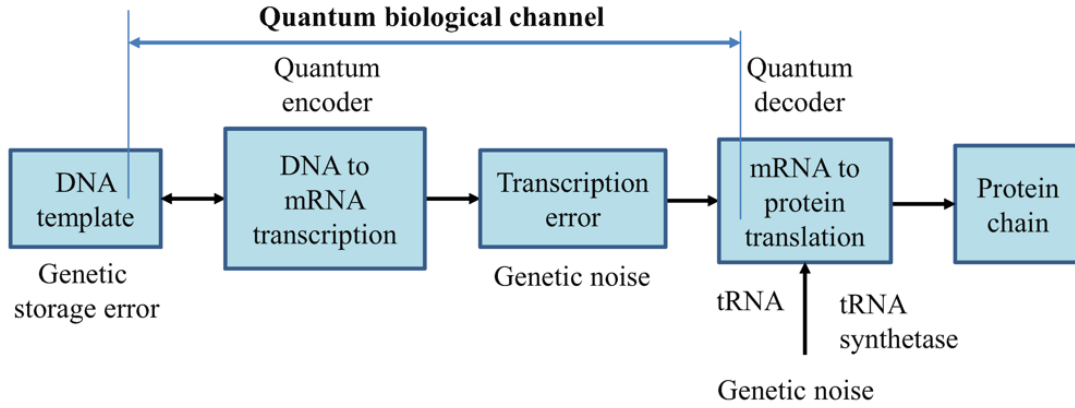


Figure 2.5: (Djordjevic [3]) Representation of the flow of information from DNA to proteins with the tools of quantum information theory

has collapsed. We will expand on this point later when we compute the capacity of the quantum channel in case of coherence at the protein side.

### 2.2.3. Operator-sum representation and capacity evaluation of the noisy quantum channel

Another contribution to the description of the information flow of DNA using quantum information theory was made by Djordjevic [3]. The main contribution of this paper was the computation of the classical capacity of the quantum channel for the flow of information from DNA to proteins. He basically extended the channel thought by Yockey for the classical case using the quantum model of Karafyllidis. The model is represented in Figure 2.5. He described transcription as an encoder and translation as the decoding process. He also extended the channel to the DNA template since here errors due to the jump of protons to the other side of the hydrogen bond can occur. In order to compute the channel capacity one has to define the action of the channel. In his paper Djordjevic computed the channel capacity for a quantum channel that introduces errors in only one nucleotide base of a codon. Defining a channel in this case means finding the transition probability that maps a specific codon  $|m\rangle$  to another  $|n\rangle$  that differs from the former for one nucleotide. This transformation is described by the Kraus operator  $E_{m,n} = \sqrt{p_{m,n}} |n\rangle \langle m|$ , where  $p_{m,n}$  is the transition probability from state  $|m\rangle$  to state  $|n\rangle$ . In Figure 2.6 is represented the transition diagram for codon AUU as effect of the quantum channel. Note that not all transitions will encode to protein different from the one corresponding to AUU, Ile. The output codon  $|n\rangle$  could be in principle one of all 64 codons (61 if we do not consider stop codons).

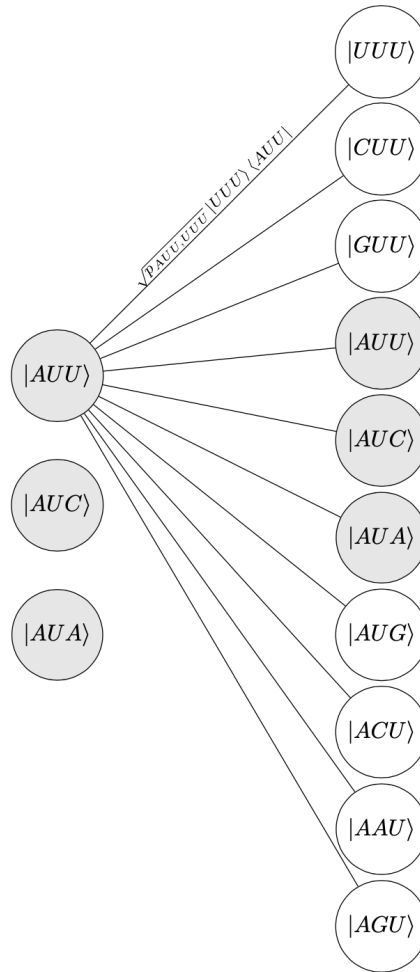


Figure 2.6: Transition diagram of codon AUU encoding the protein Ile. Underlined circles represent codons that encode Ile.  $p_{m,n}$  represent the transition probability from basket  $|m\rangle$  to  $|n\rangle$ .

Since we assume that only transitions with one different nucleotide are permitted, there are at most nine different transitions from the started codon. In Table D.1 of Appendix D, we show all the possible transitions due to the action of the channel for each codon sent from the transmitter.

Concerning the input source, Djordjevic considered three cases:

1. a set of twenty completely mixed states of codons encoding the same protein. The density operator of a generic input is then  $\rho_a = \sum_m p_m |m\rangle \langle m|$ . For instance, for the protein Ile, we have the ensemble of codons  $m \in \{AUU, AUA, AUC\}$ , and  $\rho_a = \frac{1}{3} \sum_m |m\rangle \langle m|$ ;
2. the state encoding a protein, is a superposition of eigenkets of the protein's Hamil-

tonian. For Phe we have:

$$|\psi\rangle = a(|\text{UUC}\rangle + |\text{UUU}\rangle) + b(|\text{UUC}\rangle - |\text{UUU}\rangle). \quad (2.8)$$

if the coefficients are equal, i.e.,  $a = b = \frac{1}{\sqrt{2}}$ , then  $|\psi\rangle = |\text{UUC}\rangle$ . And this is true for each input state;

3. is selected on eigeket at random for each input from the protein's Hamiltonian.

It is interesting to note that the first case incorporates the degeneracy of the genetic code into itself. A more intuitive way to think about degeneracy is in this term. Suppose that our source is actually a set of 61 orthogonal equiprobable states representing all the possible codons:  $\rho = \sum_m p(m) |m\rangle \langle m|$  with  $p(m) = 1/61$ . In order to simulate degeneracy we can think that the receiver can project the arrival states only in 20 states. Define for each amino acid  $a$ ,  $\mathcal{S}_a = \{m : m \text{ codes } a\}$  and  $d_a = |\mathcal{S}_a|$ . We can define the projectors

$$P_a = \sum_{m \in \mathcal{S}_a} |m\rangle \langle m|. \quad (2.9)$$

$P_a$  are orthogonal and  $\sum_a P_a = I$ . We can apply those projectors to our input state  $\rho$ :

$$\rho_s = \sum_a P_a \rho P_a^\dagger = \sum_a P_a \left( \frac{1}{61} \sum_m |m\rangle \langle m| \right) P_a^\dagger = \sum_a \frac{1}{61} \sum_{m \in \mathcal{S}_a} |m\rangle \langle m|. \quad (2.10)$$

Note now that the probability of the generic codon  $m$  can be written as  $1/61 = p(m) = p(m|a)p(a) = p(a)/d_a$ , than:

$$\sum_a \frac{p(a)}{d_a} \sum_{m \in \mathcal{S}_a} |m\rangle \langle m| = \sum_a p_a \rho_a, \quad (2.11)$$

That is the same notation used by Djordjevic.

The action of the quantum biological channel is then defined by the map

$$\mathcal{E}(\rho_s) = \sum_{m,n} E_{m,n} \rho_s E_{m,n}^\dagger. \quad (2.12)$$

A quantum operation CPTP (completely positive and trace-preserving) is defined if and only if the Kraus operators satisfy the completeness relation  $\sum_{m,n} E_{m,n}^\dagger E_{m,n} = I$ .

This condition guarantees that the transition probabilities sum to one. Since we consider erased the transitions to the stop codons there will be some input  $|m'\rangle$  for which  $\sum_n E_{m',n}^\dagger E_{m',n} < I$ , leading  $\mathcal{E}$  to be a non-trace preserving map. Of course this map can be extended to CPTP maps by adding extra Kraus operators  $E_{m,r} = \sqrt{p_{m,n}} |r\rangle \langle m|$  such that for each input  $|m'\rangle$  we have  $\sum_n E_{m',n}^\dagger E_{m',n} = I$ .

We know that a quantum operation satisfying the completeness relation is a physically possible operation. From our set of Kraus operators it is possible to find a model environmental system and dynamics that give rise to such a set of Kraus operators. Suppose we have an isometry acting as  $V : \mathcal{H}_S \otimes |e_0\rangle \rightarrow \mathcal{H}_S \otimes \mathcal{H}_E$  defined as:

$$V(|m\rangle |e_0\rangle) = \sum_n E_{m,n} |m\rangle_S |m, n\rangle_E, \quad (2.13)$$

where  $|e_0\rangle$  is some standard state of the environment. It is easy to see that thanks to the completeness of the Kraus operators, for each  $|\psi\rangle = \sum_{m'} \alpha_{m'} |m'\rangle$  and  $|\phi\rangle = \sum_{m''} \alpha_{m''} |m''\rangle$  we have

$$\langle \psi | \langle e_0 | V^\dagger V | \phi \rangle | e_0 \rangle = \langle \psi | \phi \rangle. \quad (2.14)$$

Then  $V$  can be extended to a unitary  $U : \mathcal{H}_S \otimes \mathcal{H}_E \rightarrow \mathcal{H}_S \otimes \mathcal{H}_E$  [12, ex. 2.67]. Such  $U$  can be represented as the block matrix

$$U = \begin{bmatrix} [E_1] & \cdot & \cdot & \cdot & \cdot & \cdots \\ [E_2] & \cdot & \cdot & \cdot & \cdot & \cdots \\ [E_3] & \cdot & \cdot & \cdot & \cdot & \cdots \\ [E_4] & \cdot & \cdot & \cdot & \cdot & \cdots \\ \vdots & \vdots & \vdots & \vdots & \vdots & \ddots \end{bmatrix} \quad (2.15)$$

in the basis  $|m, n\rangle_E$ . The Kraus operators determine only the first column. The rest represent the extension from  $V$  to  $U$  and is up to us (in Appendix A we show the relation between the unitary of eq. (2.15) and the map of eq. (2.12)).

In order to compute the capacity of the quantum channel defined by the Kraus operators Djorjevic employs the HSW theorem:

$$C(\rho_s) = \max_{\{p_j, \rho_j\}} \left[ S \left[ \mathcal{E} \left( \sum_j p_j \rho_j \right) \right] - \sum_j p_j S(\mathcal{E}(\rho_j)) \right], \quad (2.16)$$

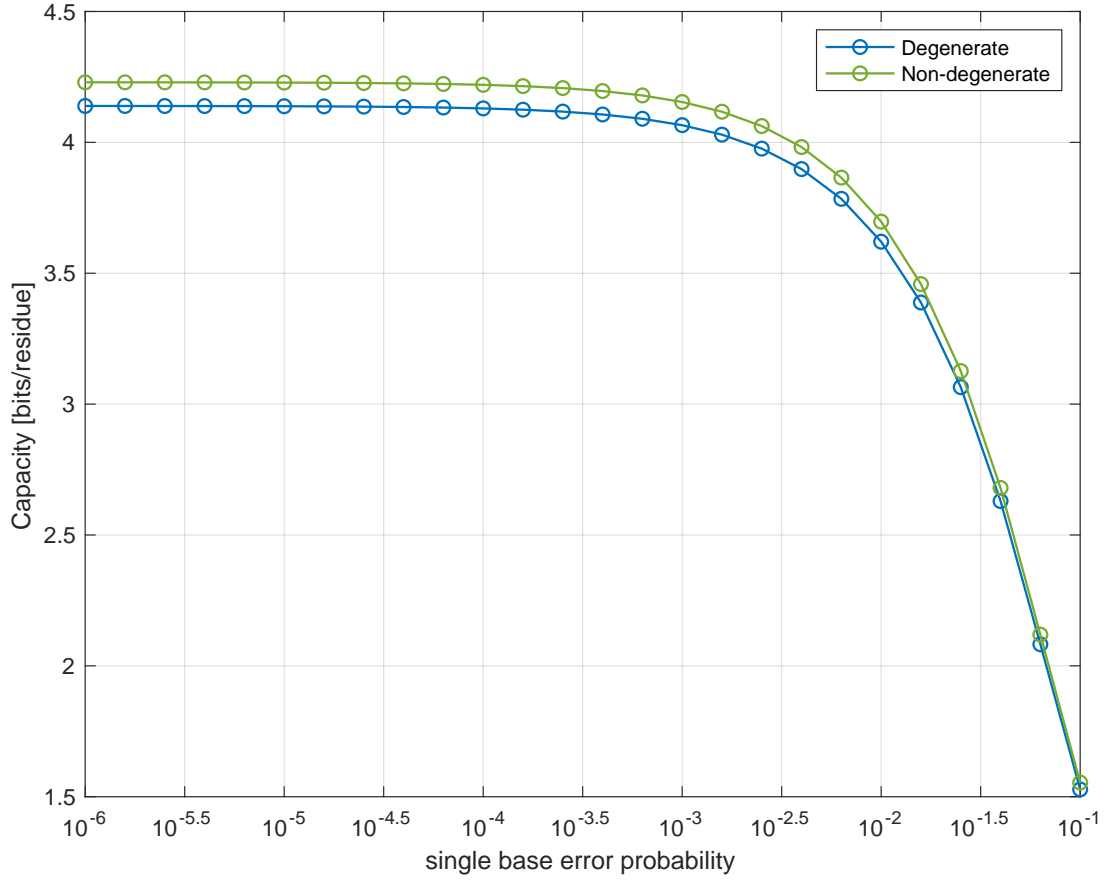


Figure 2.7: Capacity of the biological channel against the single base error probability. The blue line represents the case in which the eigenvalues of the Hamiltonian at the protein side are degenerate, leading to a higher loss of information with respect to the case when the eigenvalues of the Hamiltonian are not degenerate, represented here by the green line.

where  $\rho_s = \sum_j p_j \rho_j$ . Of course the capacity is defined as performing a maximization over all the ensemble  $\{p_j, \rho_j\}$ . But if we assume a uniform input distribution of the codons we cannot choose an arbitrary distribution  $\{p_j\}$ . Figure 2.7 depicts the capacity calculation with equation (2.16) of the map  $\mathcal{E}$  of equation (2.12) in the case of 1. for the characterization of the source by the blue line.

### 2.3. Alternative quantum biological channel for DNA flow of information

### 2.3.1. Channel convex decomposition

The quantum biological channel defined by Djordjevic, describes the possible change from a state representing a codon to a state representing a codon that differs from the sent one for one nucleotide base. We have already said that if we don't consider stop codons, there are at most nine different error transitions for each baseket, see Table D.1. Considering all the possible transitions (including the correct ones) we count a total of  $K = 587$  Kraus operators of the form  $E_{m,n} = \sqrt{p_{m,n}} |n\rangle \langle m|$ . We have used  $K$  to indicate the total number of Kraus operators. More precisely  $K$  is called the *Kraus rank*, that is, the minimum number of Kraus operators that describe its corresponding completely positive map  $\mathcal{E} = \sum_k E_k \rho E_k^\dagger$  [4].  $K$  is also called *Choi rank* because its number is the same as the rank of the *Choi matrix*  $J(\mathcal{E})$  associated with  $\mathcal{E}$ . Since  $J(\mathcal{E})$  in our case has dimension  $61 \cdot 61 \times 61 \cdot 61$ , the Kraus rank is at most 3721 (see Appendix B). In this section we show a method to reduce the number of Kraus operators to  $K = 10$  leading to a channel that has the same behavior as the quantum Djordjevic channel in the case of diagonal input states.

The construction of the channel starts from the transition diagram of which (2.6) is only a part. The whole transition diagram can be seen as a bipartite graph where on the left are all the possible 61 input codon states and on the right are all the possible 61 output states. Then we can connect them with edges characterized by their transition probability. A bipartite graph can be represented by a matrix whose columns represent the input (the left part of the graph) and the rows the output (the right part). Such a matrix can be easily obtained by writing:

$$M = \sum_{m,n} (E_{m,n})^2 = \sum_{m,n} p_{m,n} |n\rangle \langle m|. \quad (2.17)$$

Here the square of the Kraus operators has to be intended as the square of each element of their matrix representation. The general element in column  $m$  and row  $n$  represents the transition probability  $p_{m,n}$  from codon  $|m\rangle$  to codon  $|n\rangle$ . For each column, fixing its corresponding index we have that  $\sum_{n=1}^{61} M(m,n) \leq 1$ , if we consider that  $\sum_{m,n} E_{m,n}^\dagger E_{m,n} < I$ . The matrix  $M$  is called a *doubly sub-stochastic* matrix, i.e., a matrix with only non-negative entries and where each column and row sum at most to one.

*Theorem 2.1 ([5]):*

Let  $M$  be a doubly sub-stochastic matrix, then it can be written as a convex com-

bination of sub-permutation matrices:

$$M = \alpha_0 P_0 + \alpha_1 P_1 + \cdots + \alpha_{L-1} P_{L-1}, \quad (2.18)$$

where  $\sum_{l=0}^{L-1} \alpha_l = 1$ . Sub-permutation matrices  $P_l$  are permutation matrices with some of the ones replaced with zeros.

The bipartite graph drawn from the matrix  $M$  that describes classical transitions of codons consists of 3 properties:

1. Each input vertex is connected to eight to ten output vertices;
2. Each output vertex is connected to eight to ten input vertices;
3. If input  $m$  has output  $n$  then input  $n$  has output  $m$ .

Property 3 ensures that a specific element, says the codon  $|AAA\rangle$  has the same number of edges when it is an input or an output. All the edges, described mathematically by the Kraus operators and representing all the possible transitions of the bipartite graph, can be collected in different groups. These groups can be obtained by finding the perfect matchings of the bipartite graph, whose matrix representations are the sub-permutation matrices of equation (2.18). Perfect matchings on a bipartite graph are a collection of disjoint edges where each input incidents one output. The matrix  $M$  has in the diagonal the transition probabilities corresponding to the correct transition of the codons after the channel. The diagonal matrix will be our first permutation matrix  $P_0$ . We then define the new doubly sub-stochastic matrix  $M_1 = M - (1 - 9p)P_0$ , which has all the elements of the diagonal equal to zero - all the remaining elements describe an error after the channel, so they all have the same value  $p$ . Due to the symmetry of the bipartite graph described by the biological channel, we can find another perfect matching since Hall's condition is still valid and therefore write a new permutation matrix  $P_1$  and a new sub-stochastic matrix as  $M_2 = M_1 - pP_1$  and repeat the procedure until we will find some input vertices with no edges. This will happen after having found the permutation matrix  $P_7$ . In fact, the matrix  $M_8$  will have some columns and rows with zero elements and the Hall's condition will not be satisfied: no perfect matching will be found. However at this point input and output vertices out of edges will be the same. We can then find a perfect matching for the reduced bipartite graph and then write the other two sub-permutation matrices  $P_8$  and  $P_9$ . Excluding the mandatory permutation matrix  $P_0$ , essential for the description of the correct transition of the channel, the permutation matrices  $P_1, P_2, \dots, P_7$  could be

chosen in principle with some freedom since perfect matchings are not unique for a given structure of the bipartite graph. We change the notation of  $P$  with  $U$ , and we can write the initial doubly sub-stochastic matrix as:

$$M = (1 - p)U_0 + p \sum_{k=1}^9 U_k \quad (2.19)$$

Defining the Kraus operators  $A_k = \sqrt{p_k}U_k$ , it is easy to see that:

$$\sum_{k=0}^9 A_k^\dagger A_k < I \quad (2.20)$$

and the completely positive (non-trace preserving) map  $\mathcal{E}_c : \rho \rightarrow \rho'$  with Kraus rank  $K = 10$  is:

$$\mathcal{E}_c(\rho) = \sum_{k=0}^9 A_k \rho_s A_k^\dagger = \sum_{k=0}^9 p_k U_k \rho_s U_k^\dagger. \quad (2.21)$$

The channel  $\mathcal{E}_c(\rho)$  is said to be a convex combination of extreme channels  $\mathcal{E}_k(\rho) = U_k \rho U_k^\dagger$  (channels that cannot be decomposed into a convex combination of other channels), i.e.,  $\mathcal{E}_c(\rho_s) = \sum_k p_k \mathcal{E}_k(\rho_s)$  and can be physically interpreted as the application of the channel  $\mathcal{E}_k$  with probability  $p_k$  [7]. It is important to note that the map just found  $\mathcal{E}_c$  is not equal to  $\mathcal{E}(\rho_s) = \sum_{m,n} E_{m,n} \rho_s E_{m,n}^\dagger$ . In fact we cannot say that  $\mathcal{E}_c(\rho_s) = \mathcal{E}(\rho_s)$  for every input state  $\rho$ . Equality holds only for completely mixed states, i.e., for diagonal states. It is actually quite straightforward to find the real convex decomposition of  $\mathcal{E}$ . Indeed, we can write

$$\mathcal{E}_k = \sum_{m,n} G_{m,n}^k \rho_s (G_{m,n}^k)^\dagger, \quad G_{m,n} = |n\rangle \langle m| \quad (2.22)$$

for those  $(m,n)$  for which  $P_k(m,n) = 1$ . The necessary and sufficient condition for a channel to be extreme is that the set  $\{(G_{m,n}^k)^\dagger G_{m,n}^k\}_{m,n}$  must be linearly independent [1, 7].  $(G_{m,n}^k)^\dagger G_{m,n}^k = |m\rangle \langle n| \langle n'| \langle m'| = |m\rangle \langle m|$  and the set  $\{|m\rangle \langle m|\}_{m,n}$  is clearly linearly independent. As a consequence [1, remark 6], the Kraus rank must be  $K < 2^n$  where  $n$  is the number of qubits of the system. For general channels the bound on the Kraus rank is  $K < 2^{2n}$ .

### 2.3.2. Capacity evaluation assuming coherence at the protein side

If we consider the degeneracy of the eigenvalues at the protein side we can gain extra information as depicted by the green line in Figure 2.7. If a state  $|m\rangle$  arrives to the receiver, since it is no longer an eigenstate of the Hamiltonian, the new state will be:

$$|\psi(t)\rangle = \sum_j \langle \psi_j | m \rangle e^{-iE_j t / \hbar} |\psi_j\rangle. \quad (2.23)$$

If the measure is defined by the eigenvectors of  $H_{PROT}$ , the probability of collapse on the eigenstate  $j^*$ , i.e, the probability of measure eigenvalue  $j^*$  is:

$$p(E_{j^*}) = |\langle \psi_{j^*} | \psi(t) \rangle|^2 = \left| \sum_j \langle \psi_j | m \rangle e^{-iE_j t / \hbar} \langle \psi_{j^*} | \psi_j \rangle \right|^2 = |\langle \psi_{j^*} | m \rangle|^2. \quad (2.24)$$

So after the measure we can see the state due to  $|m\rangle$  as:

$$\rho_m = \sum_j |\langle \psi_j | m \rangle|^2 |\psi_j\rangle \langle \psi_j|. \quad (2.25)$$

If we also consider the effect of the noisy channel defined by the map  $\mathcal{E}_c$  we can write the mixed state as:

$$(1 - 9p)\rho_m + p \sum_n \rho_n.$$

If we assume that each codon is equiprobable, the capacity can be computed as:

$$\mathcal{C}(\rho) = S \left[ \frac{1}{61} \sum_{m=1}^{61} \left( (1 - 9p)\rho_m + p \sum_n \rho_n \right) \right] - \frac{1}{61} \sum_{m=1}^{61} S \left[ (1 - 9p)\rho_m + p \sum_n \rho_n \right]. \quad (2.26)$$

In Figure 2.7 the plot of the capacity computed with equation 2.26 is depicted in green.

# 3 | Quantum circuit for quantum biological channel

In this chapter, we describe how to implement the dynamics of the quantum biological channel introduced in the previous chapter on a quantum circuit. We show that its convex decomposition into extreme channels provides a convenient and efficient approach for synthesizing the overall operation in terms of elementary quantum gates. Finally, we use the resulting circuit to numerically estimate the channel capacity through a Monte Carlo simulation, showing convergence to the theoretical value as the number of trials increases.

## 3.1. Circuit construction

In the previous chapter our aim was to study the dynamics of the system transporting the genetic information when it interacts with another system, the environment. This leads us to think about the system that we are interested in obtaining information on as open quantum systems. We have seen that such dynamics can be studied using the theory of quantum operations by defining a unitary operator  $U$  acting on both systems leading to an action on the principal system described by the Kraus operators. This unitary transformation can be implemented in a quantum computer and our aim is to find a strategy to efficiently do it. In Section 2.2 we have derived a part of the unitary transformation  $U$  of equation (2.15). What was missing was the completion to the unitary. Such construction guarantees that if we have two systems where one represents the codon space and the other the environment, a general state  $|m\rangle|e_0\rangle$  will produce, after tracing out the environment, a state according to the map  $\mathcal{E}$  of equation (2.12). This approach to the problem turns out to be non-convenient. In our case  $\dim(U) = 61 \cdot 587 \times 61 \cdot 587$  and so we need a  $\lceil \log_2(61) \rceil = 6$  qubits for the principal system and  $\lceil \log_2(587) \rceil = 10$  qubits for the environment: a total of 16 qubits. Nowadays such a number leads to a CNOT count that is huge for a practical implementation of quantum circuits. There are many

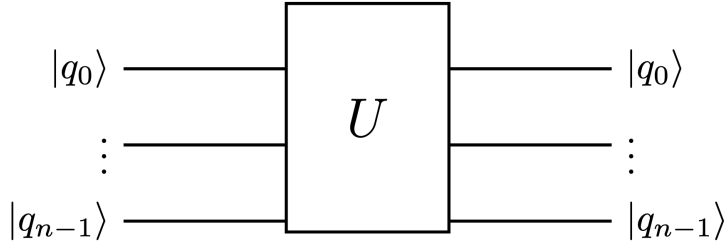


Figure 3.1: Unitary gate of  $n$  qubits acting on  $n$  qubits

algorithms that can decompose this unitary in elementary quantum gates. For example if we consider the Shannon quantum decomposition [15], the maximum number of CNOT gates needed for the synthesis is of the order  $4^n$  and in our case this is unpracticable. Even if we use the representation derived in Section 2.3 and the dimension of the environment reduces to four qubits, still a very huge number of CNOTs are needed. Note that we are taking the number of CNOTs as scarce resource. This because, with respect to single qubit gates, the implementation of CNOTs is more prone to errors [7]. So CNOT count will measure the cost of the circuit. In order to proceed we recall what was said about channels: they can be seen as a convex decomposition of extreme channels, i.e., channels that cannot be decomposed further in other extreme channels. So we can write the generic channel  $\mathcal{E}_c$  as:

$$\mathcal{E}_c = \sum_k p_k \mathcal{E}_k, \quad (3.1)$$

where  $\mathcal{E}_k$  are extreme channels. We have found that a description of the biological channel that introduces errors on one single base of a codon has a convex decomposition (here we will consider the convex decomposition  $\mathcal{E}_c$  since we consider only diagonal input states). Each extreme channel  $\mathcal{E}_k$  is defined by only one Kraus operator. So the action of the channel  $\mathcal{E}_c$  is to choose one of the deterministic  $\mathcal{E}_k$  with probability  $p_k$ . This means that for a real simulation, rather than stacking the ten Kraus operators  $A_k$  and completing the unitary, we can apply one of the operators  $U_k$  to the system according to the distribution  $p_k$ . So we just need to find a way to decompose in elementary gates the single permutation matrices. In order to do this we will exploit the method of the *Householder reflections* as described in [11]. Suppose that we have a unitary  $U$  acting on  $n$  qubits as depicted in Figure 3.1. A Householder decomposition of  $U$  means finding an operator  $G$  that is a product of elementary gates on  $n$  qubits, i.e.,  $G = G_k G_{k-1} \dots G_0$  and such that  $GU = I$ . Then  $U = G^\dagger$  and  $G_0^\dagger \dots G_{k-1}^\dagger G_k^\dagger$  is an implementation of  $U$  by a cascade of

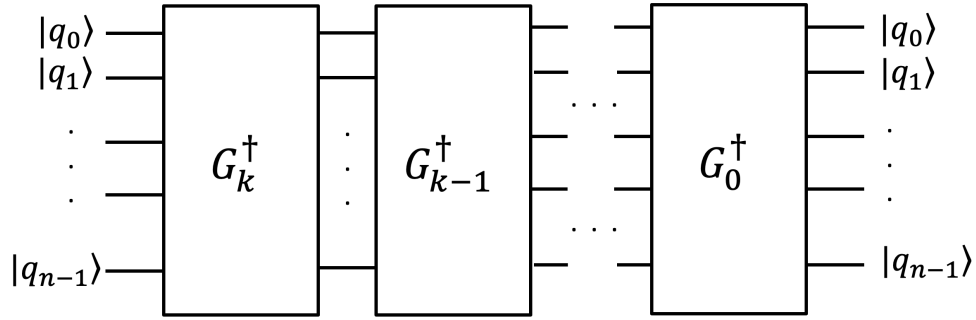


Figure 3.2: Cascade of elementary quantum gates implementing the action of a permutation operator

elementary gates, see Figure 3.2. Each  $G_i$  is a Householder reflection. We now give some useful definition for the construction of such reflections.

*Definition (state preparation):* let  $|v\rangle$  and  $|w\rangle$  be two states on  $n$  qubit. We say that a unitary  $\text{SP}_{w,v}$  implements the state preparation for  $|v\rangle$  from  $|w\rangle$  if:

$$\text{SP}_{w,v} |w\rangle = |v\rangle. \quad (3.2)$$

*Definition (Householder reflections):* given a unitary vector  $|v\rangle$ , the standard Householder reflection with respect to  $|v\rangle$  is:

$$H_v = I - 2 |v\rangle \langle v|. \quad (3.3)$$

*Lemma 1:* let  $\text{SP}_{w,v}$  denote a unitary implementing state preparation for the state  $|v\rangle$  from  $|w\rangle$  and  $H_w$  the standard Householder reflection with respect to  $|w\rangle$ . Then  $H_v = \text{SP}_{w,v} \cdot H_w \cdot \text{SP}_{w,v}^\dagger$ .

Given two states  $|v\rangle$  and  $|w\rangle$ , we can construct a gate that maps  $|v\rangle$  to  $|w\rangle$  using a standard Householder reflection defined as:

$$H_{v,w} = H_u, \quad \text{where } |u\rangle = \frac{|v\rangle - |w\rangle}{\| |v\rangle - |w\rangle \|} \quad (3.4)$$

An idea of the action of a cascade of Householder reflections to a unitary matrix is given in Figure 3.3. Let  $|v_0\rangle = U |0\rangle$  be the first column of  $U$  and consider  $H_{v_0,0}$ , the Householder reflection mapping  $|v_0\rangle$  to  $|0\rangle$  up to a phase. We can reduce the first column of  $U$  (and row

$$U \xrightarrow{H_{v_0,0}} \begin{bmatrix} * & 0 & 0 & 0 \\ 0 & * & * & * \\ 0 & * & * & * \\ 0 & * & * & * \end{bmatrix} \xrightarrow{H_{v_1,1}} \begin{bmatrix} * & 0 & 0 & 0 \\ 0 & * & 0 & 0 \\ 0 & 0 & * & * \\ 0 & 0 & * & * \end{bmatrix} \xrightarrow{H_{v_2,2}} \begin{bmatrix} * & 0 & 0 & 0 \\ 0 & * & 0 & 0 \\ 0 & 0 & * & 0 \\ 0 & 0 & 0 & * \end{bmatrix} \xrightarrow{\Delta} \begin{bmatrix} 1 & 0 & 0 & 0 \\ 0 & 1 & 0 & 0 \\ 0 & 0 & 1 & 0 \\ 0 & 0 & 0 & 1 \end{bmatrix}$$

Figure 3.3: ([11]) Idea of decomposition with Householder reflections. Here \* represent an arbitrary complex entry

by orthogonality) by applying the Householder reflection to the unitary matrix. With the same idea we can reduce all the other columns and rows; then we can apply a diagonal gate and get the identity matrix. For our purposes things become much easier. In fact our aim is to decompose permutation matrices, i.e., matrices with only one one for each column e row. What we ask for the Householder reflection is to make only swaps of columns in order to get the identity matrix. So we need to know two things: 1) which Householder reflections (swaps of columns) we need; 2) how we implement circuitally such swaps. For the first point we have to see the permutation matrix in terms of cycles. As said in [14], "Since we will be dealing only with bijective functions, i.e., permutations, we represent them using the cycle notation where a permutation is represented by disjoint cycles of variables". For example suppose that we have to reduce to the identity the permutation matrix:

$$P = \begin{bmatrix} 1 & 0 & 0 & 0 & 0 & 0 \\ 0 & 0 & 1 & 0 & 0 & 0 \\ 0 & 1 & 0 & 0 & 0 & 0 \\ 0 & 0 & 0 & 0 & 0 & 1 \\ 1 & 0 & 0 & 1 & 0 & 0 \\ 0 & 0 & 0 & 0 & 1 & 0 \end{bmatrix} = |1\rangle \langle 1| + |2\rangle \langle 3| + |3\rangle \langle 2| + |4\rangle \langle 6| + |5\rangle \langle 4| + |6\rangle \langle 5|. \quad (3.5)$$

We can represent  $P$  as cycles:  $(1, 1)(2, 3)(3, 2)(4, 5)(5, 6)(6, 4)$ . The first element of  $(\cdot, \cdot)$  represents the column (input) while the second represents the row (output). We can compress the notation into  $(1)(2, 3)(4, 5, 6)$ . This means that, to get the identity matrix, one has to leave column 1 as it is; column 2 must be swapped with column 3; column 4 with column 5 and finally, the new column 5 with column 6. In general the number of swaps (Householder reflections) needed is the length of each cycle minus one. In our

example we have three cycles with length 1, 2 and 3 respectively. In fact we need 3 reflections to obtain the identity. From an algebraic point of view, defining our reflections as  $H_{c_1, c_2}$  (the reflection that swaps column  $c_1$  with column  $c_2$ ) we can write:

$$\begin{aligned} P' &= H_{2,3}P = |1\rangle \langle 1| + |2\rangle \langle 2| + |3\rangle \langle 3| + |4\rangle \langle 6| + |5\rangle \langle 4| + |6\rangle \langle 5| \\ P'' &= H_{4,5}P' = |1\rangle \langle 1| + |2\rangle \langle 2| + |3\rangle \langle 3| + |5\rangle \langle 6| + |4\rangle \langle 4| + |6\rangle \langle 5| \\ P''' &= H_{5,6}P'' = |1\rangle \langle 1| + |2\rangle \langle 2| + |3\rangle \langle 3| + |6\rangle \langle 6| + |4\rangle \langle 4| + |5\rangle \langle 5| = I. \end{aligned}$$

Note that, as the permutation matrix to decompose is closer to being symmetric, fewer swaps (reflections) are needed to implement it. This means that when we choose the perfect matching, a more efficient choice is the one represented by a permutation matrix that is closer to being symmetric.

For what concern point 2) it is more convenient to work with a more general notation. A permutation matrix can be written as  $P = \sum_i |j(i)\rangle \langle i|$ . Kets represent rows and bras columns.  $j(\cdot)$  is the bijective function that maps  $i$  to the row where the element of column  $i$  is one. From equation 3.4, the Householder reflection mapping  $j(i) \rightarrow i$  and  $i \rightarrow j(i)$  is

$$H_{i,j(i)} = H_u, \quad \text{where } |u\rangle = \frac{|i\rangle - |j(i)\rangle}{\| |i\rangle - |j(i)\rangle \|} = \frac{1}{\sqrt{2}}(|i\rangle - |j(i)\rangle).$$

The last equality is due to the orthonormality between  $|i\rangle$  and  $|j(i)\rangle$ . We can then write  $H_{i,j(i)} = I - (|i\rangle - |j(i)\rangle)(\langle i| - \langle j(i)|)$ . It is easy to see that this reflection swaps  $|i\rangle$  and  $|j(i)\rangle$  without affecting any other column. In order to implement circuitally  $H_{i,j(i)}$  we can use lemma 1. Namely, if we want to implement such reflection, we can do it by building a unitary that maps  $|i\rangle$  to  $|u\rangle$  and the Householder reflection with respect to  $|i\rangle$ , leading to:

$$H_u = \text{SP}_{i,u} \cdot H_i \cdot \text{SP}_{i,u}^\dagger \quad (3.6)$$

First of all we build a unitary, which we call  $F$ , such that  $F|u\rangle = |i\rangle$ . In order to do this we write  $|i\rangle = |i_1 i_2 \dots i_n\rangle$  and  $|j(i)\rangle = |j_1 j_2 \dots j_n\rangle$ ; we find an index  $k$  such that  $j_k \neq i_k$ . Controlling on the  $k^{\text{th}}$  qubit we can apply at most  $n - 1$  CNOTs such that  $|j(i)\rangle \rightarrow |i_1 \dots i_{k-1} j_k i_{k+1} \dots i_n\rangle$ . This operation affects only the state  $|j(i)\rangle$  and leaves  $|i\rangle$  unchanged. This means that if we apply to  $|u\rangle$  the series of CNOTs as said, we will get a state  $|u'\rangle = \frac{1}{\sqrt{2}}(|i\rangle - X_k |i\rangle) = |i_1 \dots i_{k-1} i_{k+1} \dots i_n\rangle \frac{1}{\sqrt{2}}(|i_k\rangle - X_k |j_k\rangle)$ .  $X_k$  is the  $X$

Pauli operator (not operator) on the  $k^{th}$  qubit. Then, applying a single qubit rotation on the  $k^{th}$  qubit we map  $|u'\rangle$  to  $|i\rangle$ .

Before rotation, there are only two states in which the  $k^{th}$  qubit can be in: either  $\frac{1}{\sqrt{2}}(|0\rangle - |1\rangle)$  or  $\frac{1}{\sqrt{2}}(|1\rangle - |0\rangle)$ . In the first case we must rotate the state to  $|0\rangle$  while in the second case it must be rotated to  $|1\rangle$ . In order to do this we can use the rotation operator along  $y$  axis of the Bloch sphere:

$$R_y(\theta) = \begin{bmatrix} \cos \frac{\theta}{2} & -i \sin \frac{\theta}{2} \\ \sin \frac{\theta}{2} & \cos \frac{\theta}{2} \end{bmatrix}, \quad (3.7)$$

with the constraint that  $R_y(\theta)\frac{1}{\sqrt{2}}(|0\rangle - |1\rangle) = |0\rangle$  and  $R_y(\theta)\frac{1}{\sqrt{2}}(|1\rangle - |0\rangle) = |1\rangle$ . It is easy to see that in the first case  $\theta = \pi/4$  while in the second case  $\theta = -\pi/4$ .

Since  $F$  is unitary we can write  $|u\rangle = F^{-1}|i\rangle = F^\dagger|i\rangle$ . We call  $SP_{i,u} = F^\dagger$ . We have found the first piece of equation (3.6). For the Householder reflection with respect to a base-state  $|i\rangle$ , we have  $H_i = I - 2|i\rangle\langle i|$ . It represents a  $Z$  or  $-Z$  gate with  $n - 1$  controlled qubits. This gate has a CNOT count of at most  $16n - 24$  if one dirty ancilla is available [11]. It follows that we can do  $H_{j(i),i}$  using  $18n - 26$  CNOTs, and then the whole permutation matrix using at most  $(18n - 26)(2^n - 1)$  CNOTs. The last term is the number of reflections we have to implement to transform the permutation into the identity. Since the Householder reflections are Hermitian, we can write the decomposition of each permutation as  $U = H_{j(1),1} \dots H_{j(k),k} H_{j(k-1),k-1}$ .

As an example of the application of the Householder reflection consider a permutation that maps  $|i = 1\rangle = |000000\rangle$  to  $|j(1) = 16\rangle = |001111\rangle$ . The first step is to find the matrix  $F$  and then invert it. First, we choose the less significant qubit (the most right one),  $q_5$ , as control qubit. We apply three CNOT with targets  $q_4, q_3, q_2$ . Now have to rotate the last qubit to  $|0\rangle$  applying the rotation  $R_y(\pi/4)$ .  $H_1 = I - |1\rangle\langle 1|$  is a  $-Z$  gate with control qubit  $q_0 = q_1 = q_2 = q_3 = q_4 = 0$  and  $q_5$  as target. Then the inverse of  $F$  must applied. This sequence of gates leads to a Householder reflection that takes  $|1\rangle \rightarrow |16\rangle$  and  $|16\rangle \rightarrow |1\rangle$ . In Figure 3.4 we show the circuital representation of the operations we just mentioned. In Figure 3.5 all the transformations that change  $|000000\rangle$  to  $|001111\rangle$  up to a phase are shown.

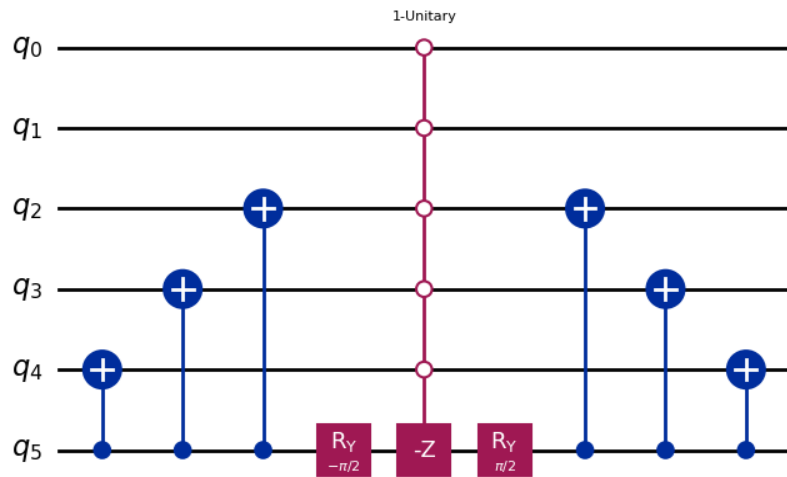


Figure 3.4: Circuit representation of the Householder reflection mapping  $|1\rangle$  to  $|16\rangle$  and  $|16\rangle$  to  $|1\rangle$

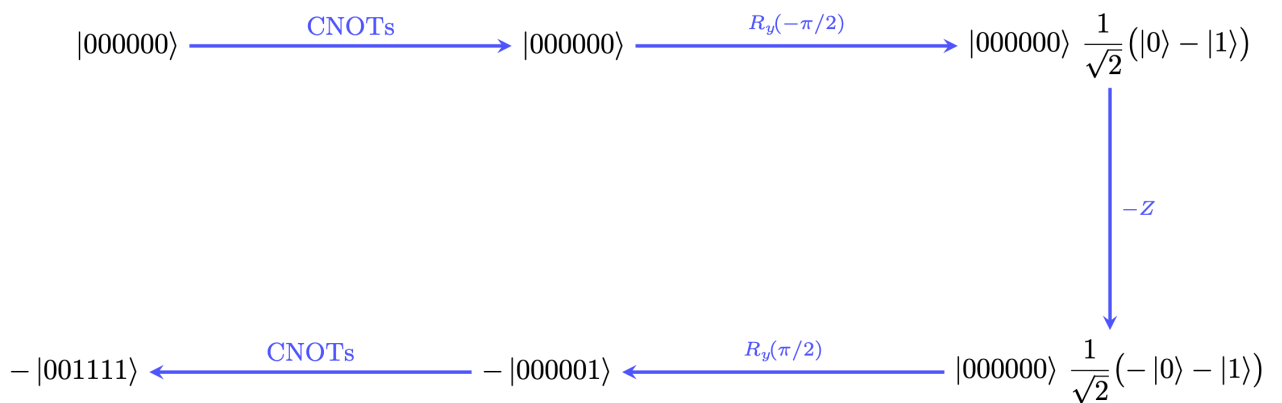


Figure 3.5: Change of the state of input  $|1\rangle$  to  $|16\rangle$  for each block of the circuit of Figure 3.4

### 3.2. Capacity evaluation

In order to compute the capacity of the biological channel with the quantum circuit we apply to an input state one of the ten permutations with its probability  $p_k$  according to equation (3.1). We are in the case where all input codons are equiprobable, i.e.  $p_i = 1/61$  with  $i = 1, 2, \dots, 61$ . For our purposes we need to know for a specific input, which permutation has been applied and in which output the state has been transformed. Note that the quantum circuits of the sub-permutations  $U_8$  and  $U_9$  were constructed after completing them, therefore starting from unitary operators. This means that there will be some transitions that are not valid. So when computing the capacity we must track them in order not to overestimate the capacity. Our data sample consists of a sequence of sent inputs, the permutation applied to those inputs and their outputs. If we get an impossible output (due to  $U_8$  or  $U_9$ ) we will mark that output as erased. Suppose that we do a simulation of  $L$  samples. The action of the channel to a generic codon  $|m\rangle$  is:

$$\mathcal{E}(|m\rangle\langle m|) = p_{m,m} |m\rangle\langle m| + \sum_n p_{m,n} |n\rangle\langle n|. \quad (3.8)$$

The transition probabilities can be computed from the data set as:

$$f_{m,n} = \frac{\# \text{ outputs } n \text{ from } m}{\# \text{ inputs } m - \# \text{ erased outputs from } m} \quad (3.9)$$

if  $L$  is large we expect that  $f_{m,n} \rightarrow p_{m,n} / (p_{m,m} + \sum_n p_{m,n})$ . We can then construct the density operators corresponding to the protein  $j$  as:

$$\mathcal{E}'(\rho_j) = \frac{1}{d_j} \sum_{m \in \mathcal{S}_j} \mathcal{E}'(|m\rangle\langle m|) = \frac{1}{d_j} \sum_{m \in \mathcal{S}_j} \left( f_{m,m} |m\rangle\langle m| + \sum_n f_{m,n} |n\rangle\langle n| \right),$$

where with  $\mathcal{E}'$  we are referring to the empiric estimation of the map  $\mathcal{E}$ , acting on a generic input  $|m\rangle$ , with  $L$  use of the channel implemented with the quantum circuit.

This kind of map leads to a capacity that is not the capacity per channel use but the capacity per "correct" use of the channel, that is, without inputs that transform into erased outputs. We can compute the former capacity by considering the total probability of erasure. The erasure does not affect all the codons but the ones that have the transitions on one or more stop codons. We can compute such a probability as

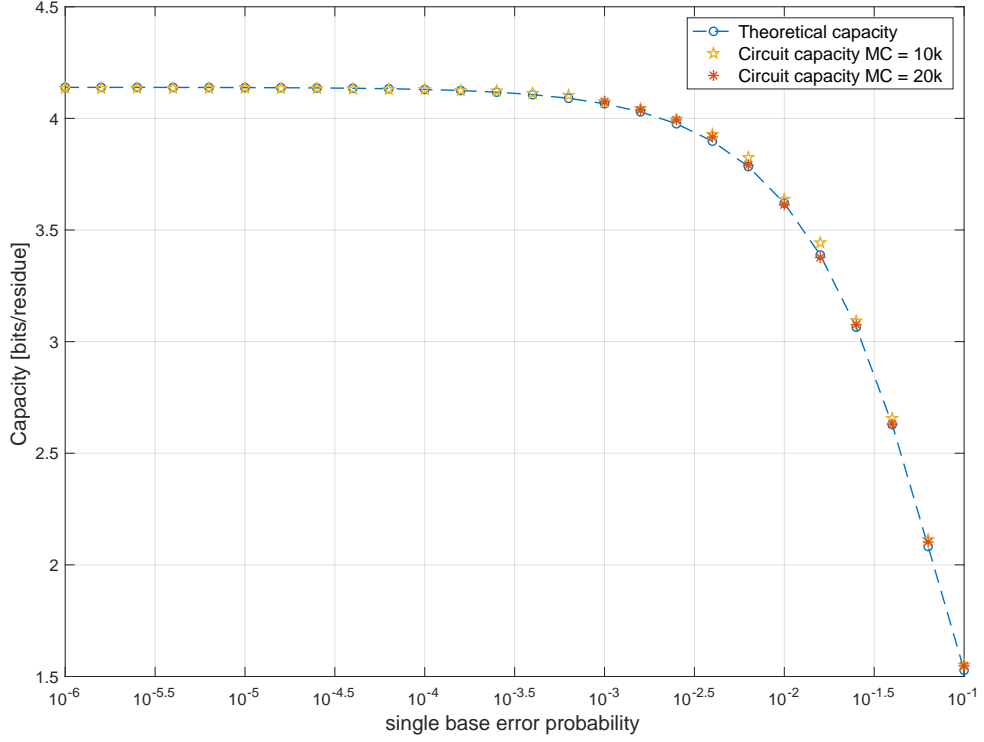


Figure 3.6: Capacity of the biological quantum channel computed with the quantum circuit.

$$p_e = \sum_m p_m p_{e|m} = \frac{1}{61} \sum_m p_{e|m},$$

where  $p_m$  is the probability of codon  $m$  and  $p_{e|m}$  is the probability of getting erased given codon  $m$ . The transition probabilities can be computed as before with the data set. Namely, once we have found the erased outputs by looking at the outputs occurring when operators  $U_8$  and  $U_9$  have been applied, we can write the frequency of erasure given the codon  $m$  as

$$f_{e,m} = \frac{\# \text{ outputs erased from } m}{\# \text{ input } m}, \quad (3.10)$$

and we expect that for a large set of data  $f_{e,m} \rightarrow p_{(e|m)}$ . For analogy we write the total frequency of erasure  $f_e$  and  $f_e \rightarrow p_e$  as the sample data get larger. Finally, we can write the capacity per channel use as

$$C = (1 - f_e)C' \quad (3.11)$$

where  $C'$  is the capacity computed through  $\mathcal{E}'$ , that is, the capacity per "correct" use of the channel. In Figure 3.6 is depicted the theoretical capacity computed in the previous chapter (blue dashed line). Red and yellow markers are the values of the capacity computed through the quantum circuit. In the case of the red markers we have used a set of  $2 \cdot 10^4$  samples, while for yellow markers we have used  $10^4$  samples. As we can see increasing the number of samples we get a better estimation of the capacity since the frequencies computed with equations (3.9) and (3.10) are closer to the actual transition probabilities.

## 4 | Conclusions

In this thesis we have presented some results that build upon the work of several authors. We have shown that the model described by Karafyllidis leads to the increasing of mutual information between DNA and proteins, since it is possible to gain more information about the source than in the classical case. From the operator-sum representation of the quantum biological channel defined by Djordjevic we have derived a convex decomposition valid for diagonal states that expresses the channel as a sum of extreme channels. These extreme channels were derived by finding the perfect matchings of the bipartite graph induced by the doubly sub-stochastic matrix associated with the 587 Kraus operators.

In general the decomposition in extreme channels for general channels is very hard to find, mostly if the dimension of the isometry defining the map is large. Once the decomposition is available, however, the dynamics are easier to implement: classical randomness can be exploited, and each extreme channel has Kraus rank  $K \leq 2^n$  (instead of the generic bound  $K \leq 2^{2n}$ ), where  $n$  is the number of qubits of the system, leading to a reduction in the synthesis cost on quantum hardware.

We have also discussed the implementation of each extreme channel, described by a permutation matrix, using the Householder reflections leading to a CNOT count of  $(18n - 26)(2^n - 1)$  if an ancilla is available. Finally, a Monte Carlo simulation was performed to validate both the correctness of the convex decomposition and the circuit implementation of each extreme channel.

Of course we must say that working with  $n = 6$  qubits, the number of CNOTs used for each permutation synthesis is still too large for a reliable implementation on a quantum circuit. Further development could be done in terms of quantum error correction in order to compensate for the non-negligible value of the fidelity of current real CNOT gates if a large number of those are used.



## Bibliography

- [1] M.-D. Choi. Completely positive linear maps on complex matrices. *Linear algebra and its applications*, 10(3):285–290, 1975.
- [2] C. Cohen-Tannoudji, B. Diu, and F. Laloe. Quantum mechanics, volume 1. *Quantum Mechanics*, 1:898, 1986.
- [3] I. B. Djordjevic. Quantum biological channel modeling and capacity calculation. *Life*, 2(4):377–391, 2012.
- [4] M. Girard, D. Leung, J. Levick, C.-K. Li, V. Paulsen, Y. T. Poon, and J. Watrous. On the mixed-unitary rank of quantum channels. *Communications in Mathematical Physics*, 394(2):919–951, 2022.
- [5] D. Hadwin and H. Radjavi. A note on mirsky’s theorem. *Linear Algebra and its Applications*, 603:186–189, 2020.
- [6] J. E. Hopcroft and R. M. Karp. An  $n^{5/2}$  algorithm for maximum matchings in bipartite graphs. *SIAM Journal on computing*, 2(4):225–231, 1973.
- [7] R. Iten, R. Colbeck, and M. Christandl. Quantum circuits for quantum channels. *Physical Review A*, 95(5):052316, 2017.
- [8] I. G. Karafyllidis. Quantum mechanical model for information transfer from dna to protein. *Biosystems*, 93(3):191–198, 2008.
- [9] P.-O. Löwdin. Proton tunneling in dna and its biological implications. *Reviews of Modern Physics*, 35(3):724, 1963.
- [10] P.-O. Löwdin. Quantum genetics and the aperiodic solid: Some aspects on the biological problems of heredity, mutations, aging, and tumors in view of the quantum theory of the dna molecule. In *Advances in quantum chemistry*, volume 2, pages 213–360. Elsevier, 1966.

- [11] E. Malvetti, R. Iten, and R. Colbeck. Quantum circuits for sparse isometries. *Quantum*, 5:412, 2021.
- [12] M. A. Nielsen and I. L. Chuang. *Quantum computation and quantum information*. Cambridge university press, 2010.
- [13] E. Schrödinger. *What is life? The physical aspect of the living cell*. Rare Treasure Editions, 2025.
- [14] V. V. Shende, A. K. Prasad, I. L. Markov, and J. P. Hayes. Synthesis of reversible logic circuits. *IEEE Transactions on Computer-Aided Design of Integrated Circuits and Systems*, 22(6):710–722, 2003.
- [15] V. V. Shende, S. S. Bullock, and I. L. Markov. Synthesis of quantum logic circuits. In *Proceedings of the 2005 Asia and South Pacific Design Automation Conference*, pages 272–275, 2005.
- [16] D. Voet, J. G. Voet, C. W. Pratt, S. Belgeri, and M. Chicca. *Fondamenti di biochimica*. Zanichelli, 2013.
- [17] H. P. Yockey. An application of information theory to the central dogma and the sequence hypothesis. *Journal of Theoretical Biology*, 46(2):369–406, 1974.

# A | Appendix A

Here we show the passages that from the unitary operator  $U$  acting on both the principal and the environment system, when we trace out the last, one gets the operator sum representation of the channel.

$$tr_E (U(\rho \otimes |e_0\rangle \langle e_0|)U^\dagger) \quad (\text{A.1})$$

Knowing that  $\rho = \sum_m p_m |m\rangle \langle m|$  and that  $(\sum_m p_m |m\rangle \langle m|) \otimes |e_0\rangle \langle e_0| = \sum_m p_m |m\rangle |e_0\rangle \langle m| \langle e_0|$ , we have:

$$\begin{aligned} U(\rho \otimes |e_0\rangle \langle e_0|)U^\dagger &= U\left(\sum_{m^*} p_{m^*} |m^*\rangle |e_0\rangle \langle m^*| \langle e_0|\right)U^\dagger = \sum_{m^*} p_{m^*} [U(|m^*\rangle |e_0\rangle \langle m^*| \langle e_0|)U^\dagger] = \\ &= \sum_{m^*} p_{m^*} \left[ \left( \sum_n E_{m^*,n} |m^*\rangle |m^*, n\rangle \right) \left( \sum_{n'} \langle m^*| \langle m^*, n'| E_{m^*,n'}^\dagger \right) \right] \end{aligned}$$

tracing out the environment  $tr_E() = \sum_{m,n} \langle m, n| () |m, n\rangle$ , we have:

$$\sum_{m,n''} \langle m, n''| \left[ \sum_{m^*} p_{m^*} \left[ \left( \sum_n E_{m^*,n} |m^*\rangle |m^*, n\rangle \right) \left( \sum_{n'} \langle m^*| \langle m^*, n'| E_{m^*,n'}^\dagger \right) \right] \right] |m, n''\rangle \quad (\text{A.2})$$

Trace is different from zero only if  $m = m^*$  e  $n = n' = n''$ . Bringing inside bra and ket only indices  $m$  e  $n$  will survive and we can write:

$$\sum_{m,n} p_m (E_{m,n} |m\rangle \langle m| E_{m,n}^\dagger) = \sum_{m,n} p_m p_{m,n} |n\rangle \langle n| \quad (\text{A.3})$$

Note that:

$$\sum_{m,n} E_{m,n} \rho E_{m,n}^\dagger \quad \rho = \sum p_m |m\rangle \langle m|. \quad (\text{A.4})$$

leads to:

$$\begin{aligned} \sum_{m,n} E_{m,n} \left( \sum_{m'} p_{m'} |m'\rangle \langle m'| \right) E_{m,n}^\dagger &= \sum_{m,n} p_{m,n} |n\rangle \langle n| \left( \sum_{m'} p_{m'} |m'\rangle \langle m'| \right) |m\rangle \langle n| = \\ &= \sum_{m,n} p_{m,n} p_m |n\rangle \langle n|. \end{aligned} \quad (\text{A.5})$$

then

$$\text{tr}_E (U(\rho \otimes |e_0\rangle \langle e_0|)U^\dagger) = \sum_{m,n} E_{m,n} \rho E_{m,n}^\dagger \quad (\text{A.6})$$

# B | Appendix B

Here we show the relation between the Choi matrix  $e$  and the Kraus rank  $K$ . Consider the state of two systems with the same dimension:  $|\alpha\rangle = \sum |i_m\rangle |m\rangle$ , then  $|\alpha\rangle \langle \alpha| = \sum_{m,m'} |i_m\rangle |m\rangle \langle i_{m'}| \langle m'|$ . Define the transformation  $J(\mathcal{E}) = (\mathcal{I} \otimes \mathcal{E})(|\alpha\rangle \langle \alpha|)$  where  $\mathcal{I}$  is the identity operator on the second system. We can write the Choi matrix as:

$$\begin{aligned} J(\mathcal{E}) &= (\mathcal{I} \otimes \mathcal{E}) \left( \sum_{m,m'} |i_m\rangle |m\rangle \langle i_{m'}| \langle m'| \right) = (\mathcal{I} \otimes \mathcal{E}) \left( \sum_{m,m'} |i_m\rangle \langle i_{m'}| \otimes |m\rangle \langle m'| \right) = \\ &= \sum_{m,m'} |i_m\rangle \langle i_{m'}| \otimes \mathcal{E}(|m\rangle \langle m'|) \end{aligned}$$

We explicitly describe the action of the channel and write:

$$J(\mathcal{E}) = \sum_{m,m'} \left[ |i_m\rangle \langle i_{m'}| \otimes \sum_{n,m''} E_{m'',n} |m\rangle \langle m'| E_{m'',n}^\dagger \right] = \quad (\text{B.1})$$

$$\sum_{m,m'} \left[ |i_m\rangle \langle i_{m'}| \otimes \sum_{n,m''} p_{m'',n} |n\rangle \langle m''|_m \langle m'|_{m''} \langle n| \right]. \quad (\text{B.2})$$

The right term is different from zero only if  $m'' = m' = m$ , then:

$$J(\mathcal{E}) = \sum_m \left[ |i_m\rangle \langle i_m| \otimes \sum_n p_{m,n} |n\rangle \langle n| \right] = \sum_m \left[ |i_m\rangle \langle i_m| \otimes \sum_n E_{m,n} |m\rangle \langle m| E_{m,n}^\dagger \right] \quad (\text{B.3})$$

$$J = \begin{bmatrix} [\sum_n p_{AUG,n} |n\rangle \langle n|] & \mathbf{0} & \mathbf{0} & \mathbf{0} & \cdots & \cdots & \mathbf{0} \\ \mathbf{0} & [\sum_n p_{UGG,n} |n\rangle \langle n|] & \mathbf{0} & \mathbf{0} & \cdots & \cdots & \mathbf{0} \\ \mathbf{0} & \mathbf{0} & [\sum_n p_{AAA,n} |n\rangle \langle n|] & \mathbf{0} & \cdots & \cdots & \mathbf{0} \\ \mathbf{0} & \mathbf{0} & \mathbf{0} & [\sum_n p_{AAG,n} |n\rangle \langle n|] & \cdots & \cdots & \mathbf{0} \\ \vdots & \vdots & \vdots & \vdots & \ddots & & \vdots \\ \vdots & \vdots & \vdots & \vdots & & \ddots & \vdots \\ \mathbf{0} & \mathbf{0} & \mathbf{0} & \mathbf{0} & \cdots & \cdots & [\sum_n p_{AGU,n} |n\rangle \langle n|] \end{bmatrix}$$

(B.4)

Each diagonal block of  $J$  is diagonal, so its rank is the number of elements on the diagonal different from zero.

# C | Appendix C

Here we show an application of the Hopcroft-Karp algorithm [6] when given the matrix  $M_7$  of Section 2.3 we have to extract the perfect matching, leading to the permutation  $P_7$  and to a sub-stochastic matrix  $M_8$  from which we can extract only a "reduced" perfect matching since some of the elements representing the same codon on both sides of the bipartite graph will be out of edges. In other words, if the  $i^{th}$  column of matrix  $M_8$  is empty, then the  $i^{th}$  row of  $M_8$  will also be empty. We will refer to the codons with the numbers as written in Table D.1.

From the matrix  $M_7$ , even by hand, we can find a matching that is represented in Table C.1 by black numbers simply by choosing for each input (column) one output (row). With this choice of the matching, inputs 49, 50, 52, 55 cannot be matched with one of their corresponding outputs since they belong to other inputs. The output codons that are not matched are 40, 42, 52, 55. In order to increase the cardinality of the matching from this scenario, we have to find an *augmenting path* that connects one of the unmatched outputs with one of the unmatched inputs. An augmenting path is a chain of edges that alternate between edges of the matching of table below and edges out of this table. The first and last edges must be out of the matching. In order to do this we draw a tree graph with at the roots the unmatched input codons as in Figure C.1 (1.). From each of them we draw a second layer that is made of all the possible outputs of each root input according to  $M_7$  (2.). The third layer consists, from each of the previous outputs, of drawing the inputs where they are currently matched (3.). The fourth layer is made by the outputs on which each input of the third layer is not connected (4.). For example, 41 can reach 41 25 55, then only 25 and 55 will be considered on third layer. Then the process restarts again creating new layers according to 1. 2. 3. and 4. until we cannot get an augmenting path connecting one unmatched root input with one unmatched output. In our case with three layers we found two augmenting paths:  $P_1 = (55, 41)(41, 1)(1, 49)$  and  $P_2 = (42, 17)(17, 18)(18, 55)$ . Then, we can do  $M \leftarrow M \oplus P_1 \oplus P_2$ , where  $M \oplus P = (M \cup P) - (M \cap P)$ . The edges on the match must be read from left to right, while the ones out of the match from right to left. Then we will have the new table with  $41 \rightarrow 55$  and  $49 \rightarrow 1$  using  $P_1$ ; and

$17 \rightarrow 42$  and  $55 \rightarrow 18$  using  $P_2$ . So note that for each augmenting path, we increase the cardinality of the match by one. In figure is also represented the augmenting path  $P_3 = (40, 11)(11, 28)(28, 44)(44, 9)(9, 50)$ . For the last augmenting path after some layers we can find  $P_4 = (60, 23)(23, 3)(3, 38)(38, 26)(26, 57)(57, 34)(34, 13)(13, 10)(10, 52)$ . In the table we represent with the green color the new matches after having added the augmenting paths. This led to finding the perfect matching that represents the permutation  $P_7$ .

We have already said that this is the last perfect matching we can find on the bipartite graph, since some codons have less than ten different neighborhoods: this is the reason why the matrix  $M$  of equation 2.17 is doubly *sub*-stochastic

**Table C.1:** Table representing the matching between codons. The general element is *input*  $\rightarrow$  *output*. The elements with output  $(\cdot)$  means that the input codon is not matched with any output. The green numbers are the new matches after having added the augmenting paths

1 $\rightarrow$ 41	17 $\rightarrow$ 18 (42)	33 $\rightarrow$ 52	49 $\rightarrow$ $(\cdot)$ (1)
2 $\rightarrow$ 58	18 $\rightarrow$ 54	34 $\rightarrow$ 13	50 $\rightarrow$ $(\cdot)$ (9)
3 $\rightarrow$ 23	19 $\rightarrow$ 7	35 $\rightarrow$ 33	51 $\rightarrow$ 17
4 $\rightarrow$ 20	20 $\rightarrow$ 6	36 $\rightarrow$ 56	52 $\rightarrow$ $(\cdot)$ (10)
5 $\rightarrow$ 19	21 $\rightarrow$ 53	37 $\rightarrow$ 25	53 $\rightarrow$ 47
6 $\rightarrow$ 27	22 $\rightarrow$ 21	38 $\rightarrow$ 26 (3)	54 $\rightarrow$ 50
7 $\rightarrow$ 57	23 $\rightarrow$ 3 (60)	39 $\rightarrow$ 37	55 $\rightarrow$ $(\cdot)$ (18)
8 $\rightarrow$ 59	24 $\rightarrow$ 36	40 $\rightarrow$ 24	56 $\rightarrow$ 32
9 $\rightarrow$ 15	25 $\rightarrow$ 29	41 $\rightarrow$ 1 (55)	57 $\rightarrow$ 34 (26)
10 $\rightarrow$ 14	26 $\rightarrow$ 5	42 $\rightarrow$ 51	58 $\rightarrow$ 2
11 $\rightarrow$ 28 (40)	27 $\rightarrow$ 39	43 $\rightarrow$ 31	59 $\rightarrow$ 8
12 $\rightarrow$ 16	28 $\rightarrow$ 48	44 $\rightarrow$ 9 (28)	60 $\rightarrow$ 38
13 $\rightarrow$ 10 (34)	29 $\rightarrow$ 46	45 $\rightarrow$ 30	61 $\rightarrow$ 4
14 $\rightarrow$ 35	30 $\rightarrow$ 45	46 $\rightarrow$ 49	/
15 $\rightarrow$ 11	31 $\rightarrow$ 43	47 $\rightarrow$ 61	/
16 $\rightarrow$ 12	32 $\rightarrow$ 44	48 $\rightarrow$ 22	/

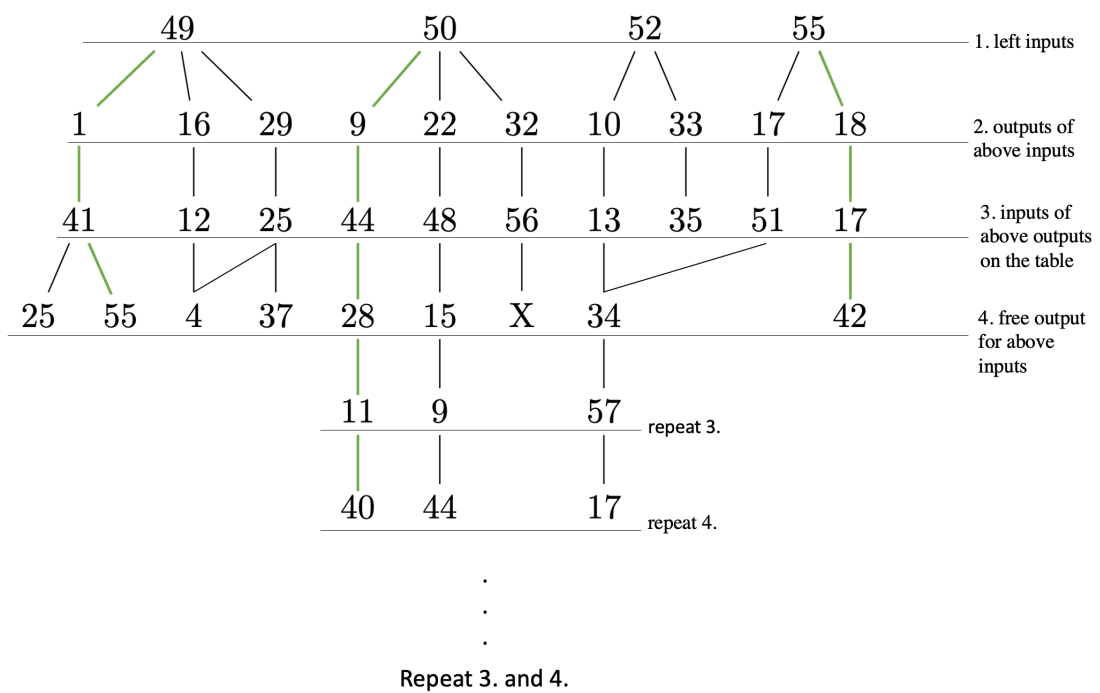


Figure C.1: Representation of the graph according to the Hopcroft–Karp algorithm. Each layer alternates edges on the match and out of the match. Green lines represent augmenting paths that connect unmatched inputs with unmatched outputs.



# D | Appendix D

Here is represented the table containing all the possible transitions for each input codon that is sent through the noisy channel. We have numbered the codons according to the order used in [8]. The codons that are not numbered are the stop codons.

Table D.1: Map of codons.

#	Codon	Tran.1	Tran.2	Tran.3	Tran.4	Tran.5	Tran.6	Tran.7	Tran.8	Tran.9
1	AUG	AAG(16)	ACG(37)	AGG(49)	AUA(22)	AUC(23)	AUU(21)	CUG(52)	GUG(41)	UUG(55)
2	UGG	AGG(49)	CGG(46)	GGG(29)	UAG	UCG(58)	UGA	UGC(7)	UGU(8)	UUG(55)
3	AAC	AAA(15)	AAG(16)	AAU(4)	ACC(38)	AGC(60)	AUC(23)	CAC(13)	GAC(5)	UAC(19)
4	AAU	AAA(15)	AAC(3)	AAG(16)	ACU(39)	AGU(61)	AUU(21)	CAU(14)	GAU(6)	UAU(20)
5	GAC	AAC(3)	CAC(13)	GAA(11)	GAG(12)	GAU(6)	GCC(26)	GGC(30)	GUC(42)	UAC(19)
6	GAU	AAU(4)	CAU(14)	GAA(11)	GAC(5)	GAG(12)	GCU(27)	GGU(31)	GUU(43)	UAU(20)
7	UGC	AGC(60)	CGC(45)	GGC(30)	UAC(19)	UCC(57)	UGA	UGG(2)	UGU(8)	UUC(17)
8	UGU	AGU(61)	CGU(47)	GGU(31)	UAU(20)	UCU(59)	UGA	UGC(7)	UGG(2)	UUU(18)
9	CAA	AAA(15)	CAC(13)	CAG(10)	CAU(14)	CCA(32)	CGA(44)	CUA(50)	GAA(11)	UAA
10	CAG	AAG(16)	CAA(9)	CAC(13)	CAU(14)	CCG(33)	CGG(46)	CUG(52)	GAG(12)	UAG
11	GAA	AAA(15)	CAA(9)	GAC(5)	GAG(12)	GAU(6)	GCA(24)	GGA(28)	GUA(40)	UAA
12	GAG	AAG(16)	CAG(10)	GAA(11)	GAC(5)	GAU(6)	GCG(25)	GGG(29)	GUG(41)	UAG
13	CAC	AAC(3)	CAA(9)	CAG(10)	CAU(14)	CCC(34)	CGC(45)	CUC(51)	GAC(5)	UAC(19)
14	CAU	AAU(4)	CAA(9)	CAC(13)	CAG(10)	CCU(35)	CGU(47)	CUU(53)	GAU(6)	UAU(20)
15	AAA	AAC(3)	AAG(16)	AAU(4)	ACA(36)	AGA(48)	AUA(22)	CAA(9)	GAA(11)	UAA
16	AAG	AAA(15)	AAC(3)	AAU(4)	ACG(37)	AGG(49)	AUG(1)	CAG(10)	GAG(12)	UAG
17	UUC	AUC(23)	CUC(51)	GUC(42)	UAC(19)	UCC(57)	UGC(7)	UUA(54)	UUG(55)	UUU(18)
18	UUU	AUU(21)	CUU(53)	GUU(43)	UAU(20)	UCU(59)	UGU(8)	UUA(54)	UUC(17)	UUG(55)
19	UAC	AAC(3)	CAC(13)	GAC(5)	UAA	UAG	UAU(20)	UCC(57)	UGC(7)	UUC(17)
20	UAU	AAU(4)	CAU(14)	GAU(6)	UAA	UAC(19)	UAG	UCU(59)	UGU(8)	UUU(18)
21	AUU	AAU(4)	ACU(39)	AGU(61)	AUA(22)	AUC(23)	AUG(1)	CUU(53)	GUU(43)	UUU(18)
22	AUA	AAA(15)	ACA(36)	AGA(48)	AUC(23)	AUG(1)	AUU(21)	CUA(50)	GUA(40)	UUA(54)
23	AUC	AAC(3)	ACC(38)	AGC(60)	AUA(22)	AUG(1)	AUU(21)	CUC(51)	GUC(42)	UUC(17)
24	GCA	ACA(36)	CCA(32)	GAA(11)	GCC(26)	GCG(25)	GCU(27)	GGA(28)	GUA(40)	UCA(56)
25	GCG	ACG(37)	CCG(33)	GAG(12)	GCA(24)	GCC(26)	GCU(27)	GGG(29)	GUG(41)	UCG(58)

Continue to the next page

Table D.1 (continue)

#	Codon	Tran.1	Tran.2	Tran.3	Tran.4	Tran.5	Tran.6	Tran.7	Tran.8	Tran.9
26	GCC	ACC(38)	CCC(34)	GAC(5)	GCA(24)	GCG(25)	GCU(27)	GGC(30)	GUC(42)	UCC(57)
27	GCU	ACU(39)	CCU(35)	GAU(6)	GCA(24)	GCC(26)	GCG(25)	GGU(31)	GUU(43)	UCU(59)
28	GGA	AGA(48)	CGA(44)	GAA(11)	GCA(24)	GGC(30)	GGG(29)	GGU(31)	GUA(40)	UGA
29	GGG	AGG(49)	CGG(46)	GAG(12)	GCG(25)	GGA(28)	GGC(30)	GGU(31)	GUG(41)	UGG(2)
30	GGC	AGC(60)	CGC(45)	GAC(5)	GCC(26)	GGA(28)	GGG(29)	GGU(31)	GUC(42)	UGC(7)
31	GGU	AGU(61)	CGU(47)	GAU(6)	GCU(27)	GGA(28)	GGC(30)	GGG(29)	GUU(43)	UGU(8)
32	CCA	ACA(36)	CAA(9)	CCC(34)	CCG(33)	CCU(35)	CGA(44)	CUA(50)	GCA(24)	UCA(56)
33	CCG	ACG(37)	CAG(10)	CCA(32)	CCC(34)	CCU(35)	CGG(46)	CUG(52)	GCG(25)	UCG(58)
34	CCC	ACC(38)	CAC(13)	CCA(32)	CCG(33)	CCU(35)	CGC(45)	CUC(51)	GCC(26)	UCC(57)
35	CCU	ACU(39)	CAU(14)	CCA(32)	CCC(34)	CCG(33)	CGU(47)	CUU(53)	GCU(27)	UCU(59)
36	ACA	AAA(15)	ACC(38)	ACG(37)	ACU(39)	AGA(48)	AUA(22)	CCA(32)	GCA(24)	UCA(56)
37	ACG	AAG(16)	ACA(36)	ACC(38)	ACU(39)	AGG(49)	AUG(1)	CCG(33)	GCG(25)	UCG(58)
38	ACC	AAC(3)	ACA(36)	ACG(37)	ACU(39)	AGC(60)	AUC(23)	CCC(34)	GCC(26)	UCC(57)
39	ACU	AAU(4)	ACA(36)	ACC(38)	ACG(37)	AGU(61)	AUU(21)	CCU(35)	GCU(27)	UCU(59)
40	GUA	AUA(22)	CUA(50)	GAA(11)	GCA(24)	GGA(28)	GUC(42)	GUG(41)	GUU(43)	UUA(54)
41	GUG	AUG(1)	CUG(52)	GAG(12)	GCG(25)	GGG(29)	GUA(40)	GUC(42)	GUU(43)	UUG(55)
42	GUC	AUC(23)	CUC(51)	GAC(5)	GCC(26)	GGC(30)	GUA(40)	GUG(41)	GUU(43)	UUC(17)
43	GUU	AUU(21)	CUU(53)	GAU(6)	GCU(27)	GGU(31)	GUA(40)	GUC(42)	GUG(41)	UUU(18)
44	CGA	AGA(48)	CAA(9)	CCA(32)	CGC(45)	CGG(46)	CGU(47)	CUA(50)	GGA(28)	UGA
45	CGC	AGC(60)	CAC(13)	CCC(34)	CGA(44)	CGG(46)	CGU(47)	CUC(51)	GGC(30)	UGC(7)
46	CGG	AGG(49)	CAG(10)	CCG(33)	CGA(44)	CGC(45)	CGU(47)	CUG(52)	GGG(29)	UGG(2)
47	CGU	AGU(61)	CAU(14)	CCU(35)	CGA(44)	CGC(45)	CGG(46)	CUU(53)	GGU(31)	UGU(8)
48	AGA	AAA(15)	ACA(36)	AGC(60)	AGG(49)	AGU(61)	AUA(22)	CGA(44)	GGA(28)	UGA
49	AGG	AAG(16)	ACG(37)	AGA(48)	AGC(60)	AGU(61)	AUG(1)	CGG(46)	GGG(29)	UGG(2)
50	CUA	AUA(22)	CAA(9)	CCA(32)	CGA(44)	CUC(51)	CUG(52)	CUU(53)	GUA(40)	UUA(54)
51	CUC	AUC(23)	CAC(13)	CCC(34)	CGC(45)	CUA(50)	CUG(52)	CUU(53)	GUC(42)	UUC(17)
52	CUG	AUG(1)	CAG(10)	CCG(33)	CGG(46)	CUA(50)	CUC(51)	CUU(53)	GUG(41)	UUG(55)
53	CUU	AUU(21)	CAU(14)	CCU(35)	CGU(47)	CUA(50)	CUC(51)	CUG(52)	GUU(43)	UUU(18)
54	UUA	AUA(22)	CUA(50)	GUA(40)	UAA	UCA(56)	UGA	UUC(17)	UUG(55)	UUU(18)
55	UUG	AUG(1)	CUG(52)	GUG(41)	UAG	UCG(58)	UGG(2)	UUA(54)	UUC(17)	UUU(18)
56	UCA	ACA(36)	CCA(32)	GCA(24)	UAA	UCC(57)	UCG(58)	UCU(59)	UGA	UUA(54)
57	UCC	ACC(38)	CCC(34)	GCC(26)	UAC(19)	UCA(56)	UCG(58)	UCU(59)	UGC(7)	UUC(17)
58	UCG	ACG(37)	CCG(33)	GCG(25)	UAG	UCA(56)	UCC(57)	UCU(59)	UGG(2)	UUG(55)
59	UCU	ACU(39)	CCU(35)	GCU(27)	UAU(20)	UCA(56)	UCC(57)	UCG(58)	UGU(8)	UUU(18)
60	AGC	AAC(3)	ACC(38)	AGA(48)	AGG(49)	AGU(61)	AUC(23)	CGC(45)	GGC(30)	UGC(7)
61	AGU	AAU(4)	ACU(39)	AGA(48)	AGC(60)	AGG(49)	AUU(21)	CGU(47)	GGU(31)	UGU(8)

## List of Figures

1.1	Graph $G$ with six vertices and six edges . . . . .	4
1.2	Example of bipartite graph. Blue edges represent a perfect matching . . . . .	5
1.3	Circuit representation for the controlled-NOT gate. The top line represents the control qubit, the bottom line the target qubit. . . . .	9
1.4	Circuit representation for the $C^n(U)$ operation, where $U$ is a unitary operator on $k$ qubits, for $n = 4$ and $k = 3$ . . . . .	10
1.5	Open quantum system consists of principal system and environment . . . . .	11
1.6	Transfer of information from DNA to itself (replication) and from DNA to protein through RNA . . . . .	15
1.7	On the left, the DNA double-helix structure is illustrated; on the right, the unwinding of DNA during the replication process is shown. . . . .	16
1.8	The genetic code . . . . .	17
2.1	Possible positions of the proton shared in the hydrogen bond . . . . .	20
2.2	Molecular structure of nucleotides. Here the pair A -T has two hydrogen bonds; C - G has three hydrogen bonds. . . . .	21
2.3	The upper figure shows a simplified representation of the nucleotides, illustrating the configuration of hydrogen bonds at the interface under standard conditions; the lower figure depicts their corresponding tautomeric forms. . . . .	21
2.4	Communication scheme that represents the transfer of information from DNA to proteins. The degeneracy of the code is considered by the degeneracy of the eigenvalues at the protein side. If coherence is assumed at the protein side, the eigenvalues are no more degenerate. . . . .	24
2.5	(Djordjevic [3]) Representation of the flow of information from DNA to proteins with the tools of quantum information theory . . . . .	26
2.6	Transition diagram of codon AUU encoding the protein Ile. Underlined circles represent codons that encode Ile. $p_{m,n}$ represent the transition probability from baseket $ m\rangle$ to $ n\rangle$ . . . . .	27

2.7	Capacity of the biological channel against the single base error probability. The blue line represents the case in which the eigenvalues of the Hamiltonian at the protein side are degenerate, leading to a higher loss of information with respect to the case when the eigenvalues of the Hamiltonian are not degenerate, represented here by the green line. . . . .	30
3.1	Unitary gate of $n$ qubits acting on $n$ qubits . . . . .	36
3.2	Cascade of elementary quantum gates implementing the action of a permutation operator . . . . .	37
3.3	([11]) Idea of decomposition with Householder reflections. Here $*$ represent an arbitrary complex entry . . . . .	38
3.4	Circuit representation of the Householder reflection mapping $ 1\rangle$ to $ 16\rangle$ and $ 16\rangle$ to $ 1\rangle$ . . . . .	41
3.5	Change of the state of input $ 1\rangle$ to $ 16\rangle$ for each block of the circuit of Figure 3.4 . . . . .	41
3.6	Capacity of the biological quantum channel computed with the quantum circuit. . . . .	43
C.1	Representation of the graph according to the Hopcroft–Karp algorithm. Each layer alternates edges on the match and out of the match. Green lines represent augmenting paths that connect unmatched inputs with unmatched outputs. . . . .	55

## List of Tables

C.1	Table representing the matching between codons. The general element is <i>input</i> $\rightarrow$ <i>output</i> . The elements with output $(\cdot)$ means that the input codon is not matched with any output. The green numbers are the new matches after having added the augmenting paths . . . . .	54
D.1	Map of codons. . . . .	57



## Acknowledgements

Beh, che dire se non ringraziare tutti quelli che durante questo percorso universitario mi sono stati vicino. Non pochi anni sono passati dall'inizio a Pisa e se mi guardo indietro vedo come questo capitolo della mia vita sia stato fatto di tanti paragrafi, alcuni conclusi, altri ancora aperti, altri abbandonati.

Tutto ciò non sarebbe comunque stato possibile senza la mia famiglia, i miei genitori e i miei fratelli. Quindi un infinito grazie va a loro, la cui vicinanza e l'affetto è sempre stato sostegno e luogo dove poter tornare.

Un altro grande grazie è per il Professor Magarini, non solo per il fatto di essere stato la mia guida per questo mio ultimo lavoro da studente, ma anche per gli anni precedenti, i cui laboratori, progetti e corsi sono state esperienze di cui posso solo farene tesoro.

Grazie anche ai miei amici, siano quelli dell'infanzia, di Pisa o di Milano: con la vostra vicinanza, la vita sa di qualcosa.

Alessandro

